Turun yliopisto
University of Turku

FORMATION OF PEROVSKITE LAYERS AND THEIR CHARACTERIZATION USING SPECTROSCOPIC METHODS

Madhu Paudyal

Thesis submitted to the faculty of the material chemistry
in partial fulfilment of the
requirements for the degree of

MASTER OF SCIENCE

In

Materials science

Turku, Finland

This thesis work was carried out at the Laboratory of Material Chemistry Research Group, University of Turku, Finland. I would like to express my sincere gratitude to all the colleagues and friends in material chemistry group.

I would like to thank my supervisor and mentor Pia Damlin, Professor Carita Kvarnström, and Mikko Salomäki, for their support throughout the period of me working in the lab. It was an absolute honor to have seen these people working and learning from them about the work ethics and me working beside them was truly above imagination.

Also, I would like to say special thanks to Rahul Yewale, Lokesh, Sachin and Bo Peng for their help and advices during the period.

Last but not the least, it's my pleasure and honor to pay my special gratitude towards Fortum foundation scholarship for granting me scholarship to carry out the research and it certainly helped a lot during my stay in Finland during the research.

Madhu Paudyal

2019, Turku

Abstract

Replacing fossil fuels with green energies has been the main area of field in energy for decades and solar energy has been leading the way. Currently the evolution of perovskite solar cell (PSC) within the photovoltaic research field has certainly changed the way forward. Quick development of efficiency from 4% to above 22% is due to its band-gap tunability which makes perovskite materials interesting for use in photovoltaic solar cells.

This thesis explores the photo physics of perovskite material by focusing on development of its different processes like electrodeposition, spin coating, dip coating and ultrasonic spray coating.

Secondly, comparison of the perovskites formed using different formation procedures were done using spectroscopic methods like Raman spectroscopy and UV-Vis spectroscopy. The degradation of the perovskite layers relative to humidity and moisture present in atmospheric air was evaluated and some experiments were performed to have an idea of how the degradation affected on material properties.

Finally, Poly (methyl methacrylate) (PMMA) was deposited on the top of the perovskite layer which was introduced for the prevention of perovskite layer from moisture and atmospheric humidity.

Key words: Perovskite, Spin Coating, Ultrasonic spray coating, Electrodeposition, PMMA

Abbreviations

PHJ= Planar Heterojunction

PEC= Power Conversion Efficiency

HTL= Hole Transporting Layer

ETL= Electron Transporting Layer

PCBM = [6,6]-phenyl-C61-butyric acid methyl ester

PEDOT: PSS= Poly(3,4-ethylenedioxythiophene) Polystyrene Sulfonate

MAPI= Methylammonium Lead Iodide

DMSO= Dimethyl sulfoxide

DMF= Dimethylformamide

GBL= Gamma-Butyrolactone

FTO= Fluorine-doped Tin Oxide

BBL= Poly(benzimidazobenzophenanthroline)

MAI= Methylammonium Iodide (CH_3NH_3I)

HI= Hydrogen Iodide

PMMA= Polymethyl Methacrylate

List of Figures

Contents

Table of Contents

1. Introduction

1.1 Need of Solar cells

Due to the requirement of more green energy for the society to be as high as 1 GW/day and the supply range being not enough for the demand of 1GW/day; evolution of more renewable sources like solar energy has to be more appreciated[1]. The most direct approach for the use of solar energy is the use of photovoltaics which also benefits from the lower land usage and less infrastructure along with the reduction of visual impact that is the drawback with many other renewable technologies[1,2].

The rapid use and evolution of solar cells has been promising as the main source of energy for foreseeable future and different types of solar cells have been contributing their part for progressive development of solar energy lead by silicon based solar cells. However, recent development of perovskite solar cell in lab in 2009 had certainly diverted the studies done in this field[3,4] .

1.1.1 *Solar cell history*

Evolution of solar cells recently have to be acknowledged but the efficiency management on those solar cells have always been a factor to assess the development of the cell itself. Since 1950s, the imagination of generation of electricity from solar photo voltaic was there and research was conducted for several decades focusing on silicon technology. Although silicon solar cells have been dominating the landscape of photovoltaics, future of this cell looks to be deemed because of its high fundamental cost barriers, such as high temperature processing. The progression of solar cells has been discussed further for convenience of the understanding of its transformation with time[5,6].

1.1.1.1 First generation solar cells

Concept of solar cell was thought of during 1950s and the research was focused mainly on the use of silicon-based device structure with PN junction with p-type and n-type doped silicon regions. Silicon cell certainly do have efficiency of over 25% with real world module efficiency of around 21-22%. Silicon cell currently dominates the solar energy market with over 80 % share and recent oversupply of silicon PV from China has deducted cost to $0.50/watt from $2/watt has certainly hindered the progress of new technology to compete and have their market

share growing [6]. However, the requirement of high-grade silicon is the hinderance which is currently being over shadowed by the flexibility in the area of use on roof tops and its maximum power production compensating for the expensive factor.

Recent studies on silicon-based PV technology no longer focuses on improvement of the ~~on the~~ absolute efficiency since the record efficiency obtained by crystalline and multi-crystalline silicon cells were obtained 1999 and 2004, respectively in the lab and since then difference in real life efficiency and lab efficiency is getting smaller[7].

1.1.1.2 Second generation solar cells

This generation of solar cell was based upon the thin film solar cells and it was encouraged by the deficiency of silicon which was its indirect band gap which resulted in the low absorption coefficient and requiring the layers of around ~100 µm. Thin film solar cells with good photovoltaic properties like cadmium telluride (CdTe) and copper indium gallium selenide (CIGS) could result the similar absorption with ~1 µm thickness.

This technology certainly has its market share behind silicon based solar cells and it's been based upon the PN-junction architecture and thin layer of cadmium sulphide acting as the n-type material. Efficiency of this generation of solar cell would be around 14% in the theory which results of around 12.8% in operation[7].

1.1.1.3 Third generation solar cells

Third generation of solar cells do compose of different material use including, nanotubes, silicon wires, solar inks using conventional printing press technologies, and conductive plastics organic, quantum dot and dye sensitized solar cells along with multi junction solar cells too. Although commercial aspect of this technology has been low the promise is there for emerging market for the future. First cell of this generation was created on 1990s with dye sensitized solar cells operating through biomimetic process which was similar to the photosynthesis[8,9].

To improve on the solar cells already commercially available, this has to be more efficient over a wider band of solar energy (e.g., including infrared) and less expensive so it can be used by more and more section of market people which will certainly result in the further development of its technology and use cases. However, third generation solar cells are being based only in the laboratory.

Dye sensitized solar cell as a representation of this era have reached 14% in the lab which is certainly low than traditional silicon solar cells but its use of low-cost abundant materials and very good response in diffuse light conditions certainly promises the further research and developments in those materials.

The main factor which is obstructing the progress of these material is their instability resulting on the corrosion of the material used leaking of volatile solvent present in the electrolyte used for its development. Therefore, the use of solid electrolyte has been emphasized and heavily doped organic hole conducting material like Spiro-OMeTAD. The practical efficiency of these solar cells could not exceed 8 % and thickness of only ~2 μm has been suggested for optimum efficiency but the light absorption on that case will be so low for its commercial use[9] .

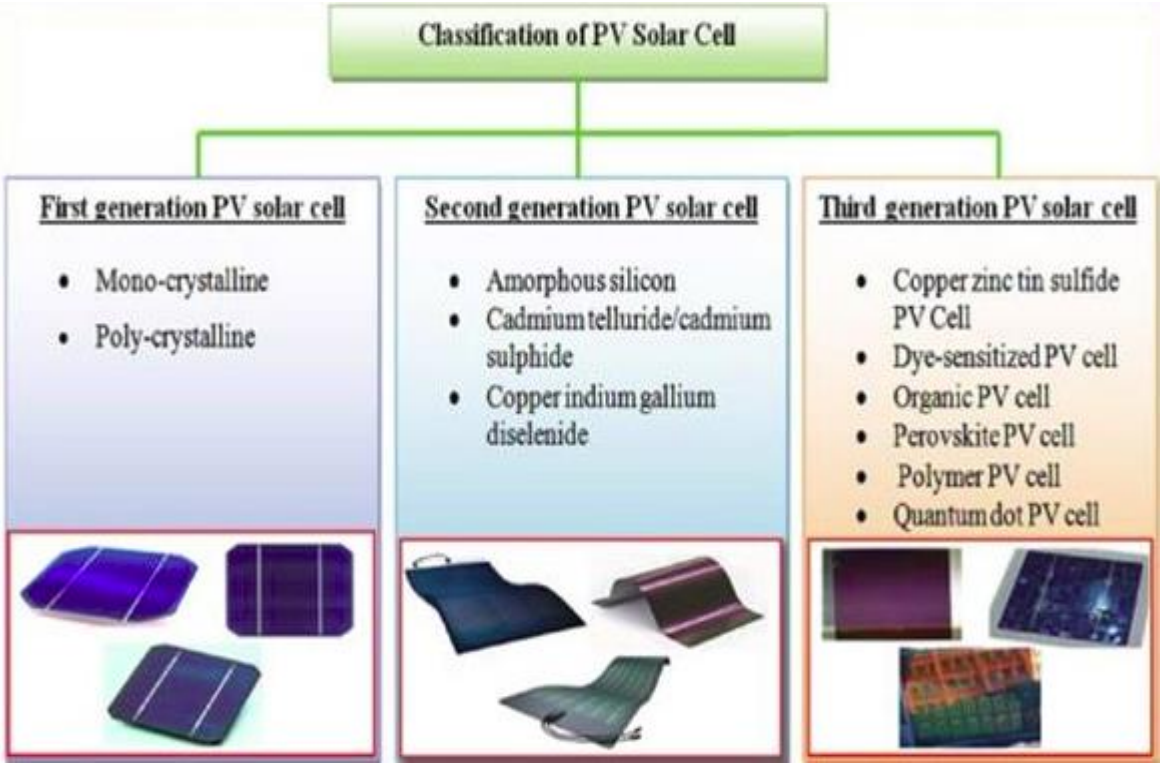

Figure 1 : Evolution of solar cell [10]

1.2 Perovskites

Even though perovskite was first discovered by Gustav Rose in 1839, the utilization of it on solar cells just begins years ago. Perovskite originally means the calcium titanium oxide mineral composed of calcium titanate ($CaTiO_3$). It is named after a Russian mineralogist Lev Perovski (1792–1856). In 1926, a Norwegian mineralogist, Victor Goldschmidt, discovered the perovskite crystal structure in his work on tolerance factors.

In 1945, Helen Dick Megaw published the crystal structure of it from X-ray diffraction data on barium titanate.[13] Nowadays, people use the term perovskite to represent material with similar cubic Pm3m framework structure of composition ABX_3.

1.2.1 *Intrinsic properties of perovskite*

Structure that perovskite poses is the structure of ABX_3 crystal structure and the Figure 2 gives the illustration of ABX_3 crystal structure. The structure can be explained as the cubic unit with the red spheres representing negatively charged X atoms whereas black dot in the center of the cubic stands for B atom which are normally smaller-sized metal cations (lead) which are positively charged and blue balls represents larger-sized metal cations(CH_3NH_3) which are mostly favored to balance the charge of the structure[11].

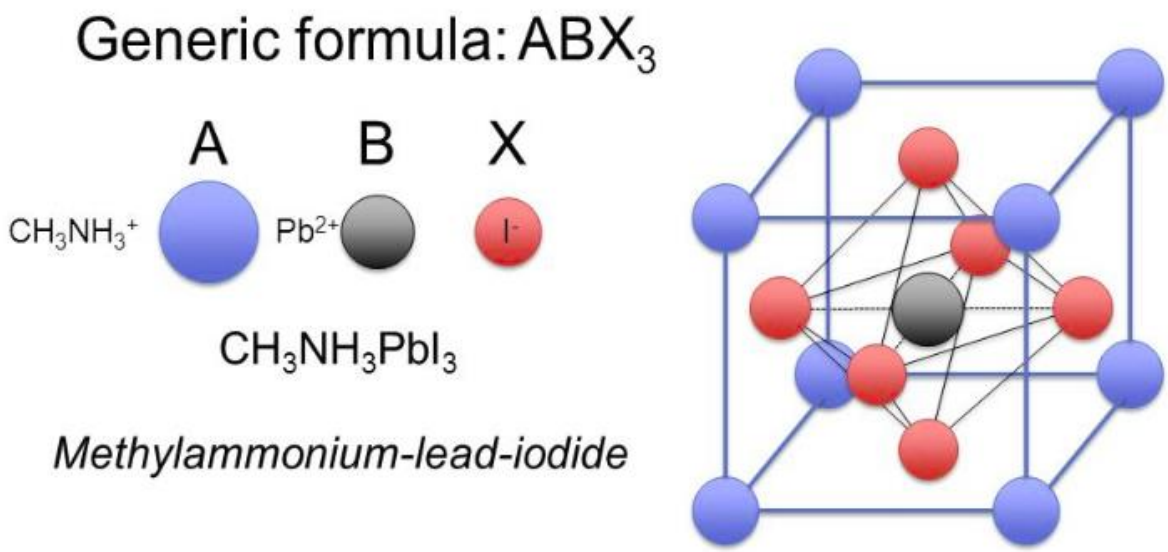

Figure 2: Structure of ABX_3 crystal[12]

A is commonly coordinated with 12 X anions and B is coordinated with 6 X anions. Extending the cubic to multiple units, one can tell the BX_6 octahedra are corner- connected to form an octahedron. The hinged octahedra allow for wide adjustment of the B-X-B bond angle[15].

For solar energy harvesting, inorganic-organic perovskite is the most popular one among its kind. A-site atoms of this kind of perovskite are replaced by organic positively charged groups. Methylammonium lead iodide ($CH_3NH_3PbI_3$ or $MAPbI_3$ or simply MAPI) and its derivatives are currently being studied and wildly used in many different research groups.

$MAPbI_3$ have a relatively small forbidden bandwidth (energy gap) around 1.5eV [15]which makes it promising in solar cell. Although it is not as ideal as silicon who has a band gap energy of 1.1eV, it is much easier to make perovskite solar cells than to make a silicon-based one to distort from their regular positions. Iodide have a larger ionic radius (2.2Å) with six- fold coordination than bromide (1.96Å), thus the BX_6 octahedron in $MAPbI_3$ is distorted while the $MAPbBr_3$ owns regular ones. Relatively more stable structure gives $MAPbBr_3$ a higher band gap energy (2.2eV).

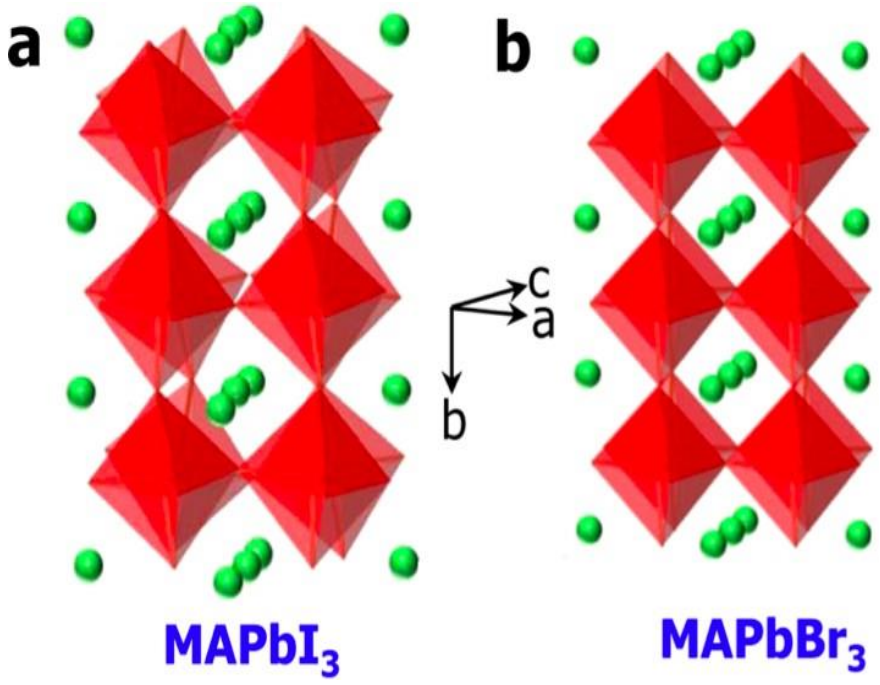

Figure 3: (a) Distorted perovskite structure of $MAPbI_3$ at room temperature; (b) Cubic perovskite structure of $MaPbBr_3$ at room temperature[13]

By adjusting the ratio of iodide and bromide in perovskite MAPb $(I_xBr_{1-x})_3$, the efficiency change of solar cell products can be observed. When x rising from 0 to 0.2, the efficiency of perovskite solar cell increases, and it start to drop down when x is beyond 0.2. Also, keep the environmental conditions the same, the most stable perovskite is obtained when x equals 0.2. The change of energy band gap of MAPb $(I_xBr_{1-x})_3$ also shows a linear relationship with x [11].

1.2.2 *Perovskite-based Solar Cells*

Perovskite emergence and the idea behind its use in solar cell is the great innovation itself and in matter of few years of research it has already been considered the future. However, there are many aspects of it which needs much more studies for its continuous progress as implicated by the rapid increase in its efficiency from 3 % to 22 % by manipulating the number of electrons in different layer of the cell.

PSC advantages is their easy preparation from solution-based materials using low cost starting materials. As a result of easy manufacturing methods, these solar cells manufacture is advantage. The development of perovskite solar cells has been very rapid and the efficiencies of these cells have improved in the first cells (year 2009) from 3.8% to new cells to over 21%. The underlying development is to improve the quality of materials used, equipment optimization of the structure and the development of different manufacturing methods[2,14].

Working principle of perovskite based solar cell:

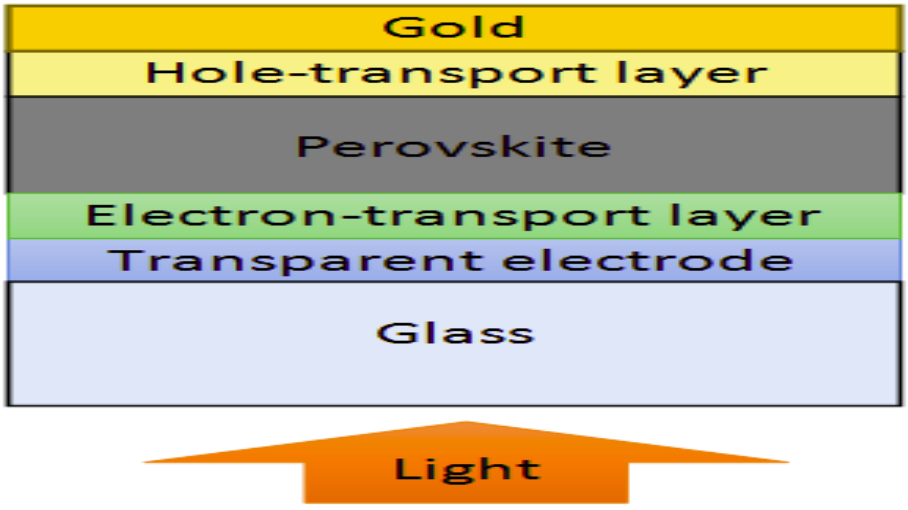

Figure 4: Illustration of silicon-based solar cell [56]

Doping atoms with more electrons than base material atom (Donor) makes the impurity semiconductor a n-type semiconductor and when doping with atoms with less electrons than base material (Acceptor) it is called p type semiconductor. After the doping of silicon n-type silicon have more electrons while the p-type silicon owns more vacant sites (holes) for the electrons to move around in the cell. This interface of n and p doped semiconductor p-n junction.

When any sort of energy, in this case photon energy, hits the cell electrons in n-type silicon gets excited from ground state to become electronically activated and some excited electrons ends with heat energy whereas some activated ones gets attracted towards the p junction and fill the holes in the semiconductor. Since this movement is a continuing one the movement of electrons inside the cell creates the potential difference in the cell. When external electric circuit is connected and electrons from n-type silicon start to flow to the p-type silicon via it due to the potential difference. The current is collected and converted to electricity.

These multi-junction cells have been giving the highest efficiency for sure along with the higher expenditure than silicon-based solar cell and makes it extremely difficult to continue to implement this into the commercial aspect followed by the silicon solar cell the next one with high efficiency cells are perovskite solar cells have a really close efficiency comparing to it. However, lower expense for manufacturing and prototype business make perovskite solar cell more appealing than traditional one.

Years ago, scientists noticed that the perovskite have a good potential to harvest energy from sun for its high diffusion length, broad light absorption range as well as a high coefficient of absorption [1-4], and the study of perovskite solar cell soars since. The first attempt to build a solar cell using perovskites on TiO_2 was reported in 2009. With a power conversion efficiency (PEC) of 3.8%, the group succeeded.[5] After years of research, the PEC of perovskite-based cell has reached over 20% and that gives it a promising future.

Perovskite solar cells have two types of structures: meso-superstructure and planar heterojunction (PHJ). Although they share a common structure like a sandwich, planer heterojunction of perovskite solar is not the same as silicon-based one. Perovskite replace p-n junction comparing to traditional one and the working mechanism are different.

Figure (5) shows the structure of meso-superstructure perovskite solar cell. In this kind, perovskite is infiltrated into a layer of metal oxide scaffold. In order to get this product, high temperature sintering is often required. Thus, lead to the fact that it cannot be used in flexible substrates. On the other hand, PHJ perovskite solar cell is more researched because it concurs the problem with meso-superstructure solar cell by having a perovskite layer between holes[1,15].

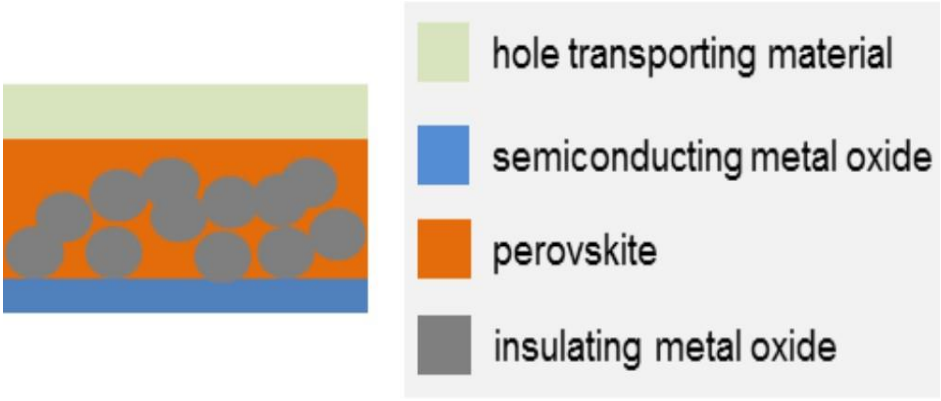

Figure 5: Meso-superstructure solar cell [58]

1.3 Manufacturing processes

In this section of the thesis, general introduction of the manufacturing process of the perovskite has been provided. There were mainly four different types of perovskite formation procedures as:

1.3.1 *Spin coating*

Spin coating is a commonly used coating technique with which smooth and covered perovskite layers can be produced. In this type of coating, the substrate to be coated is attached to a rotatable substrate and then desired amount of precursor solution is dropped on the surface of the substrate followed by the rotating the substrate which allows the precursor solution to spread evenly over the substrate on the surface with the effect of centrifugal force and at the same time the excess solution flies the plate away from the edges [16,17].

During rotation, the solvent evaporates and the perovskite crystallizes resulting in the formation of uniform perovskite layer. The coating process can be repeated several times, to produce thicker or multilayer coatings. The plating may also follow after-treatment steps such as annealing.

Annealing helps to stabilize the perovskite formation and clearly visible layer of perovskite could be seen after this. During this thesis, Spin coating technique was used to prepare film of perovskite directly with the deposition of perovskite solution manually. Detailed information about the solution and the procedure is explained in the experimental part[17].

1.3.2 *Electrochemical deposition*

Electrochemical deposition also known as electroplating involves passing electric current through a solution (electrolyte) by dipping two terminals (electrodes) into the electrolyte and connecting them into a circuit with a battery or other power supply. The electrodes and electrolyte are made from carefully chosen elements or compounds. In brief, electroplating is a process that uses electric current to reduce dissolved metal cations so that they form a thin coherent metal coating on an electrode as designated by the process. This technique is often used to change or enhance the surface properties of a target material. When the electricity flows through the circuit, the breakdown of the electrolyte takes place forming different anions and cations and the metals atoms during the process is deposited as a thin layer on top of one of the electrodes[18].

In this thesis, Lead dioxide electroplating was done for one of the steps on the manufacturing process (electrochemical deposition) of perovskite on glass sample. Further details will be discussed in the experimental section. In this process, spin coating is also one of the techniques to obtain a thin layer of absorber (PEDOT: PSS) followed by the electrodeposition technique.

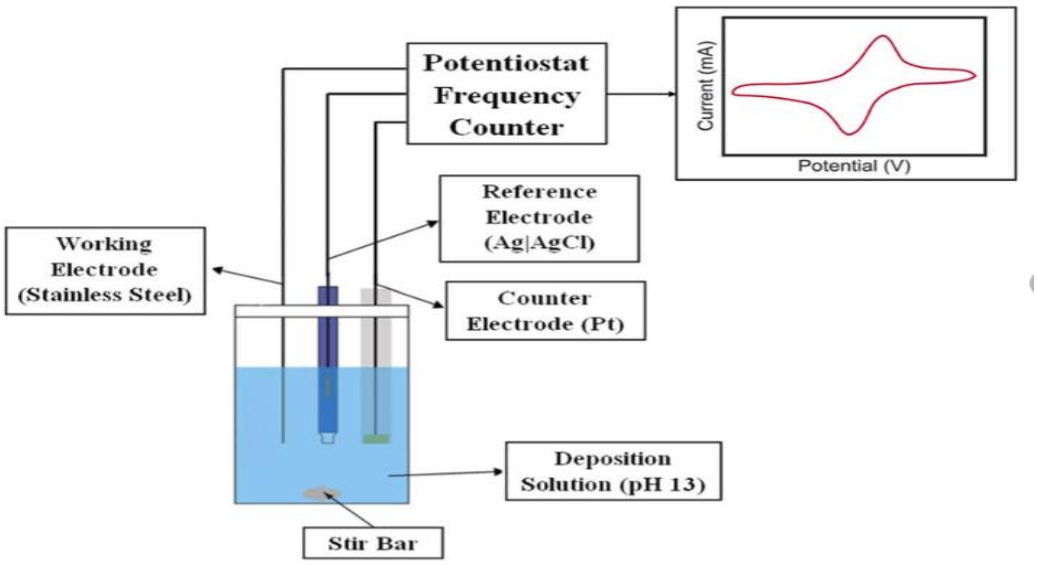

Figure 6: Schematic diagram of electrochemical deposition[19]

1.3.3 *Ultrasonic spray coating*

Spraying technology is also commonly used method to produce smooth and uniform layers, such as with drop shrinkage. Ultrasonic spray coating is a diffusion technique based on piezoelectric elements that are oscillated at a high frequency (20 kHz-3 MHz). Piezoelectric material is a material that shall be electrically polarized if subjected to mechanical stress. Similarly, in an external electric field, the piezoelectric material can be modified shape and vibrate. Nozzle of the sprayer present in the equipment is vibrated through which the liquid flows and is deposited on the surface of the target material. Affordability and suitability for large-scale manufacturing and the manufacturing efficiency are the main factors that are advantageous to this procedure. Efficient use of starting materials and good control of coating also impacts the manufacturing procedure involved.

In this thesis, Perovskite solution was ultrasonically sprayed on the top of the FTO surface and after the spraying, annealing was done in vacuum oven for the preparation of highly uniform and stable perovskite film.

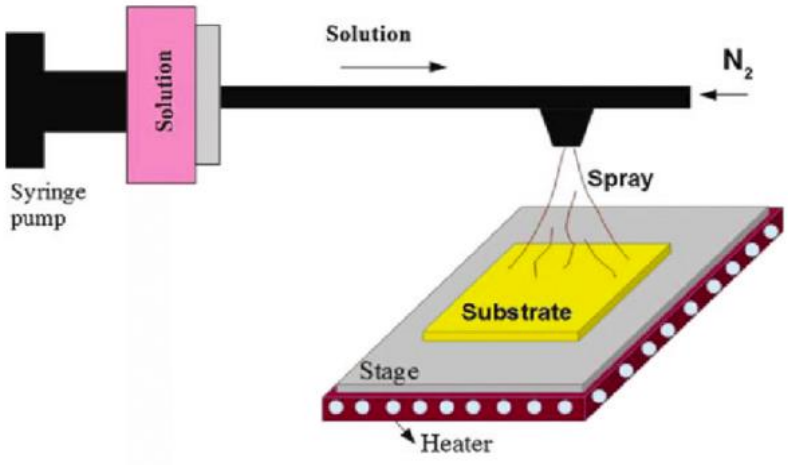

Figure 7: Mechanism of ultrasonic spray coating[20]

1.3.4 *Dip coating*

The main principle behind this procedure is to submerge the samples into HI solution. But the experiment cannot be easily controlled because of the high acidity of HI. Too concentrated solution can convert the film in a very short time and cannot be precisely controlled whereas if the concentration is too low, the conversion can be a long progress.

At one point, the film would be partly peeled off from the substrate while other parts remaining unconverted. The crucial part of this method is adjusting the concentration and time of conversion. In this research, FTO glass was dipped in the perovskite solution manually and after the process was completed it is introduced to the vacuum oven condition for annealing .

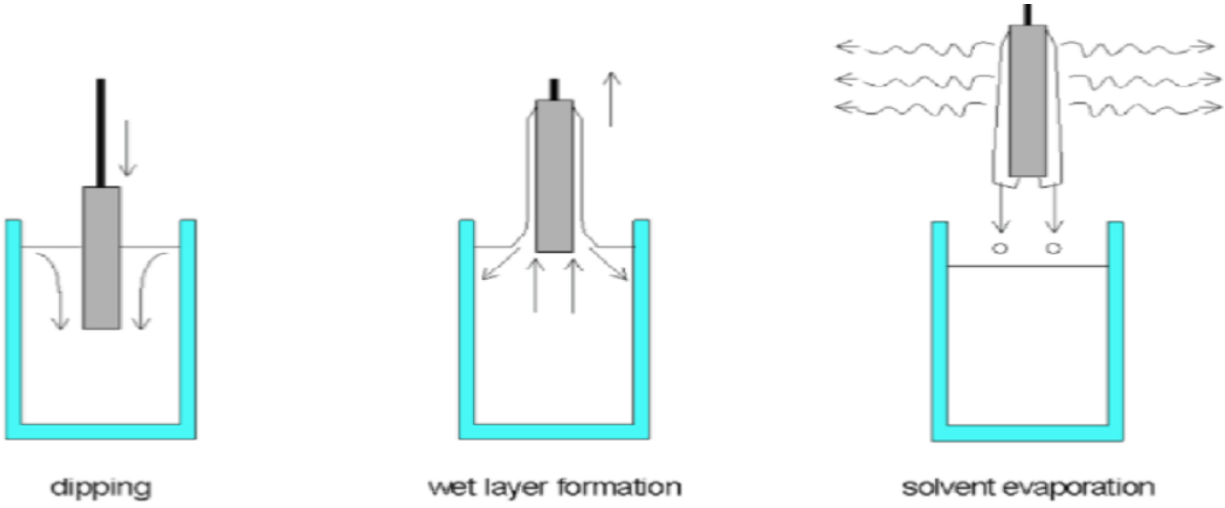

Figure 8: Schematic representation of dip coating[21]

1.4 Drawbacks of hybrid solar cells

Main concerns that are holding the commercial aspect of the perovskite are its stability and degradation. Many encapsulation techniques like UV exposure, oxygen exposure and moisture penetration has been tried and been successful for the incremental improvement of the stability to over a year after production which is however not yet commercially competitive enough as compared to the 25 years of stability of silicon based solar cells.

One of the main obstacles one may encounter when working with organic-inorganic hybrid perovskite is the easy decomposing feature. It is crucial for researchers whoever working on this material to find a way to keep it stable. The initiations of hybrid perovskite decomposition are mainly moisture, heat and light. Although light and heat also contribute to the degradation, water is the most critical one. Even though sometimes water can actually enhance the efficiency of perovskite solar cells, it is still not wanted in most of the cases. The reason why hybrid perovskite is unstable is because of its low crystal formation energy and hydroscopic nature.

Actually, alongside the initiation of degradation of $MAPbI_3$ during the reaction, there is another reaction happening where MAPI absorbs water and forms the structure of $MAPI.H_2O$, this process is reversible. Thus, by drying process, $MAPI.H_2O$ can lose the water and become pristine material again. However, it is with a limitation of within 5-10% area of perovskite degradation. The above phenomenon of MAPI degrading can only be observed when exposing long enough to moisture. Divertingly, the degradation is not exactly the same when exposing the crystal to a relatively high humidity environment or to water directly. The black color of MAPI would turn to light yellow, which is the color of lead iodide, almost simultaneously when contacting water. In this process, MAPI is degraded to PbI_2 and methyl ammonium iodide (MAI), the pristine reactants of preparing MAPI. In this process, water deprotonates $CH_3NH_3^+$ and make the reaction happen to form material with a wider band.

Current researches about the optimization of the stability of hybrid perovskite and the efficiency of its solar cell product can be concluded into three different manipulations. First, better control of the morphology of the perovskite film; second, modifications upon the reactants of perovskite; careful choice of solvent treatment.

For first method, many diverse techniques were used to control the morphology of perovskite film. For MAPI, the size of crystals has a huge influence on the sensitivity to moisture. It is because of the place where water molecules get in and start decomposing the material is the crystal grain boundaries. The decomposition goes along the in-plain direction and it is initiated at the grain boundaries. Between two crystal grains, exists an amorphous intergranular layer with a thickness around 5nm [16] and it is that layer makes water quickly diffused into the film of perovskite. The grain boundaries can be significantly adjusted by many high-tech film making techniques; thus, the efficiency of perovskite solar cell can be improved [2,22].

1.5 Characterization

In order to verify if the product synthesized is the product that was expected, spectroscopy techniques like Raman and UV- Vis was performed and further characterization and explanations were done.

1.5.1 *Raman spectroscopy and microscopy*

Raman spectroscopy is a non-destructive chemical analysis technique method based on scattering of light from the sample. This spectroscopic method provides detailed information about chemical structure, phase and polymorph, crystallinity and molecular interactions. It can also explain the interaction of light with the chemical bonds within a material.

Raman is a light scattering technique where high intensity laser light source hits the sample and light is scattered from the sample giving chemical and physical properties related to the sample. Most of the scattered light is at the same wavelength (or color) as the laser source and does not provide useful information – this is called Rayleigh scattering whereas a small amount of light (typically 0.0000001%) is scattered at different wavelengths ,which depend on the chemical structure of the analyte – this is called Raman scattering which features a number of peaks, showing the intensity and wavelength position of the Raman scattered light. Each peak corresponds to a specific molecular bond vibration, including individual bonds such as C-C, C=C, N-O, C-H etc., and groups of bonds such as benzene ring breathing mode, polymer chain vibrations, lattice modes, etc[23,24].

Raman spectroscopy with respective to the chemical structure of sample provides information about:

- Chemical structure and identity
- Phase and polymorphism
- Intrinsic stress/strain
- Contamination and impurity[25].

Thus, Raman spectrum is a typical chemical fingerprint for a particular molecule or material, and can be used to very quickly identify the material, or distinguish it from others. Raman spectral libraries are often used for identification of a material based on its Raman spectrum which contains thousands of spectra, are rapidly searched to find a match with the spectrum of the analyte[26].

1.5.2 *Ultraviolet- visible (UV-Vis) spectroscopy*

Absorption spectroscopies refer to the analysis of the radiation absorbed by a sample and it includes ultraviolet/visible light absorption (UV/Vis) atomic absorption (AA) spectroscopy, and Fourier transform infrared (FTIR) spectroscopy.

UV-Vis spectroscopy is a technique used to determine analyte concentration either at one time or often over a desired time period with the absorption of light across the ultraviolet and visible light wavelengths through a liquid sample.

Samples are dispensed into cuvette and placed in the path between a UV-Vis light and a detector. According to Beer-Lambert's law, with a constant light path length and known absorption coefficient (dependent upon wavelength), the concentration of a compound in question can be determined from the light absorbed by the sample at that wavelength. UV- vis spectroscopic analysis can be used for Quantitation of analytes, Quality assurance and control Maximum wavelength determination[27,28].

Conveniences of using UV-Vis spectroscopy is its quick and simple sample analysis and can be used for a wide variety of analytes. This spectroscopic method is much simpler than chromatographic techniques because of its user-friendly interface and requirement of very little maintenance. However, the process is subject to fluctuations from stray light and temperature changes along with relatively low sensitivity as well.
Other sample components present in the sample may also cause interferences and this technique is not as specific as chromatography and also requires relatively large sample volume, > 0.2 mL[29].

1.6 Protection of perovskite layer

Stability, cost and processing are the factors that need to be looked at during the process of manufacturing of the perovskite and researches that are conducted these days have been mostly involved for increasing Photovoltaic conversion efficiency (PCE) however, stability is the factor that has impacted (delayed) the outdoor applicability of the perovskite formed.
As discussed in the degradation part of the thesis, moisture and humidity are the main reasons for the degradation of the perovskite layer. Polymer layer if it does not directly react with the perovskite but can be used for the further layering process can be used to avoid the direct impact of humidity and moisture to the perovskite layer. Instead polymer prevents the impact which can allow the stability of the perovskite layer is increased[30].

2. Experimental

The main objective behind this thesis is to find a low-cost, efficiency and easy manufacturing method of hybrid perovskite layer on FTO substrate, study its degradation mechanism and also apply a polymer layer to delay or prevent the degradation from the factors affecting the degradation. Different manufacturing techniques are used to prepare the perovskite layer and theoretical study was done for studying degradation along with practically noticing the degradation and finally introduces a polymer layer to prevent the degradation and characterize the final sample.

2.1 Framework

The focus of this research is on the preparation of perovskite layer of organic-inorganic hybrid perovskite solar cell using various methods and examination of the properties using different spectroscopic methods. This research can be summarized to consist of three different steps. The first step is to use different methods for formation of perovskite layer on substrates such as FTO and simple glass, second step is the formation of protecting layer, polymethyl methacrylate (PMMA) layer on top of the formed perovskite layer and the final step is to characterize the layers (both with and without PMMA) using different spectroscopic methods.

The use of any hole blocking layer, in this case poly(3,4-ethylenedioxythiophene) polystyrene sulfonate (PEDOT:PSS) layer was established only for the electrochemical deposition process. Instead of PEDOT: PSS, direct deposition of perovskite layer was performed on top of FTO surface during spin coating, dip coating and ultrasonic spray coating processes for the convenience of experiments on perovskite stability itself.

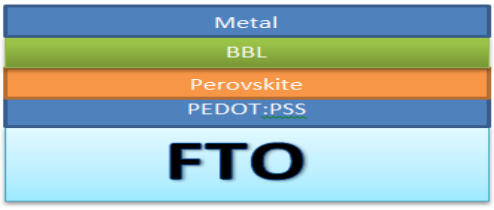

Figure 9: Basic framework of solar cell using perovskite

However, this thesis revolves around the preparation of perovskite layer and coating it with the polymer layer of PMMA as in figure below.

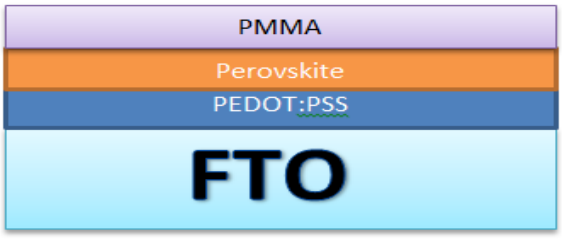

Figure 10: Basic framework of this these

For most part of the thesis, experiments were performed with FTO as a substrate as the studies was a follow up from the previous studies and comparing the research results with the previous research. It can be clearly seen that FTO was chosen as the substrate for deposition as it is transparent and it was coated with PEDOT: PSS or directly perovskite for different deposition techniques. This coating was followed by the polymer layer on top of it for its preservation and different spectroscopic methods were used for studying the degradation and also the impact of polymer layer on the degradation.

For all type of manufacturing method perovskite solution was prepared and was used with same concentration.

Cleaning of the substrate

This step was followed in each and every procedure for obtaining the optimum quality of perovskite coatings on the FTO sample. In order to make the surface of substrate more hydrophilic and easier for consecutive layers to be, samples were sanitized using acetone, ethanol and distilled water for 10 min each in ultrasonic bath. After finalizing the basic cleaning, samples were introduced to plasma cleaner for detailed surface sterilizing.

Preparation of Perovskite solution

Perovskite solution was prepared on the solvent based method from perovskite solution which was prepared from $CH_3NH_3PbI_3$, which was just a mixture of CH_3NH_3I (0.01M) and PbI_2 (0.01M) using either Dimethyl formamide (DMF) (~ 153 ° C) or Dimethylsuphoxide (DMSO) (~ 189 ° C). The concentration of the precursor solution used was 10 m-percent. Solution used for this thesis was perovskite solution of PbI_2: CH_3NH_3I (1:1) in DMF (100 ml) solution[31]

Following are the methods that were used for deposition techniques in this thesis:

2.1.1 *Spin coating*

Spin coating is a coating technique which can be used to produce smooth and covered coating layers (perovskite layers) where the substrate to be coated is attached to a rotatable substrate and then desired amount of precursor solution is dropped on the surface of the substrate followed by the rotating the substrate .This will allow the precursor solution to spread evenly over the substrate on the surface with the effect of centrifugal force and the coatings can be established on the surface of the sample[16,17].

History of spin coating started from the coatings of paint and pitch around 1958 as Emslie et al. developed the first spin coating model. This model has been used as the basis for future models and developments. The schematics of spin coating is described as the wafer in the equipment is held to chuck with vacuum pump and lid is placed over spinning basin before spin is initiated[3,17].

Perovskite solution, prepared in the lab was spin coated on FTO coated substrate by dropping the perovskite solution from pipette at 3000 rpm for 15 seconds in normal ambient temperature and subsequently annealed at 80° C for 20 min in vacuum oven. After the completion of annealing process and letting it cool for about 10 min, the morphological studies were done by Raman microscope and spectroscopy.

Basic framework of spin coating process can be categorized as:
I. Depositing fluid in the substrate (Loading)

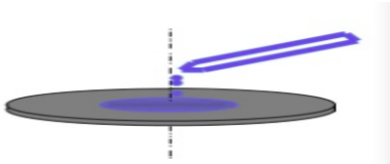

II. Acceleration of the wafer system (Dispense)

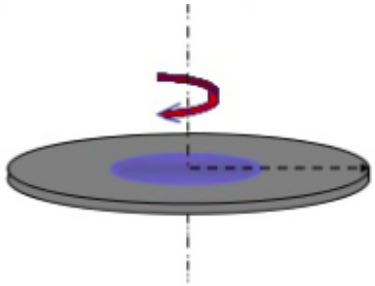

III. Coating thins at a rate that depends on the velocity of wafer and viscosity of the liquid and evaporation of liquid (Film casting)

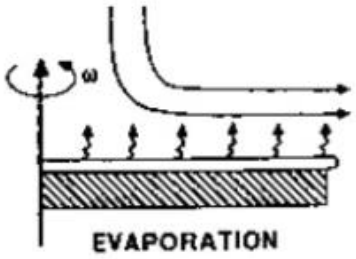

IV. Annealing (Drying)

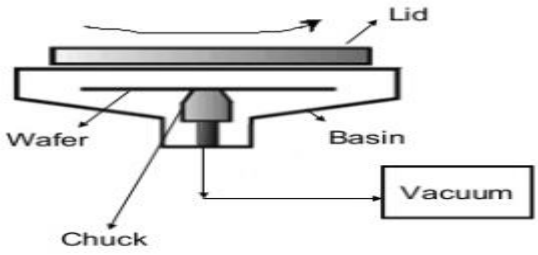

Figure 11: Principle of spin coating mechanism[32]

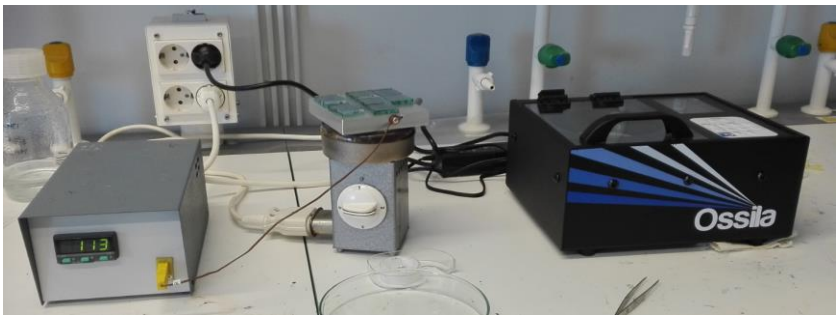

Figure 12: Spin coating system (Turku university 2018)

2.1.2 *Electrochemical deposition*

Electrochemical deposition technique works on the basic of electroplating and electroplating can be defined as the process that uses electric current to reduce dissolved metal cations in the electrolyte and transfer of that metal atom to desired electrode to form a thin coherent metal coating. This technique is often used to change or enhance the surface properties of a target material. However, in this thesis, lead dioxide was coated on top of PEDOT: PSS layer in FTO substrate[18,33].

Thin film solar cells have direct optical band gap and high absorption coefficients in visible solar spectrum. Generally named as electrodeposition, it is mainly a reduction process which attains dynamic equilibrium when metal cations, electrons are deposited at the surface of the cathode.

Parameters in which the electrodeposition is dependent upon are listed as:

- Metal, solvent and electrolyte: electronic properties of the metal surface, polar solvent (in this case aqueous solution) and the electrolyte used.
- Rate of electrodeposition: it basically is the concentration of the cations present which moves to the cathodic region. Generally, electrodeposition follows the equation of rate constant equation

  $$K = k.B.\ Th\ ln\ (-\Delta Ge.R.\ T)$$

  $$\Delta Ge = f(E)$$

  where k is rate constant, ΔGe is chemical activation energy which is a function of electrode potential E.
- Nucleation of growth mechanism: this is the process which represents the formation of layer from ions reaches the surface of the electrode and reduces nuclei at the surface to grow with respective to the parameters used.
- Structure, physical and chemical properties of electrodeposited material. In this case the deposited material is lead dioxide and elemental composition of lead dioxide will certainly impact the physical surface properties of the coated film. The properties include mechanical, electrical, optical and also reactivity and stability of the lead dioxide formed on the top of PEDOT: PSS[18,19].

Steps

Electrodeposition used for the thesis was involved in the process of formation of lead dioxide. Electrodeposition solely has not been used in the thesis for perovskite preparation process but only for the preparation of light absorbing layer perovskite through the route of electrodeposition of lead iodide followed by its conversion to lead iodide and concluding to perovskite formation at the end on top of layer of PEDOT: PSS. However, it is a process following the spin coating of PEDOT: PSS and followed by the conversion of lead dioxide to lead iodide

Initially, sample electrode is respectively cleaned in acetone, ethanol and deionized water for 10 min each and after the solvent based cleaning, the glass samples were dried and introduced to the process of plasma cleaning which eradicates any micro elements that could hinder the uniform formation of coating on the surface of the sample material.

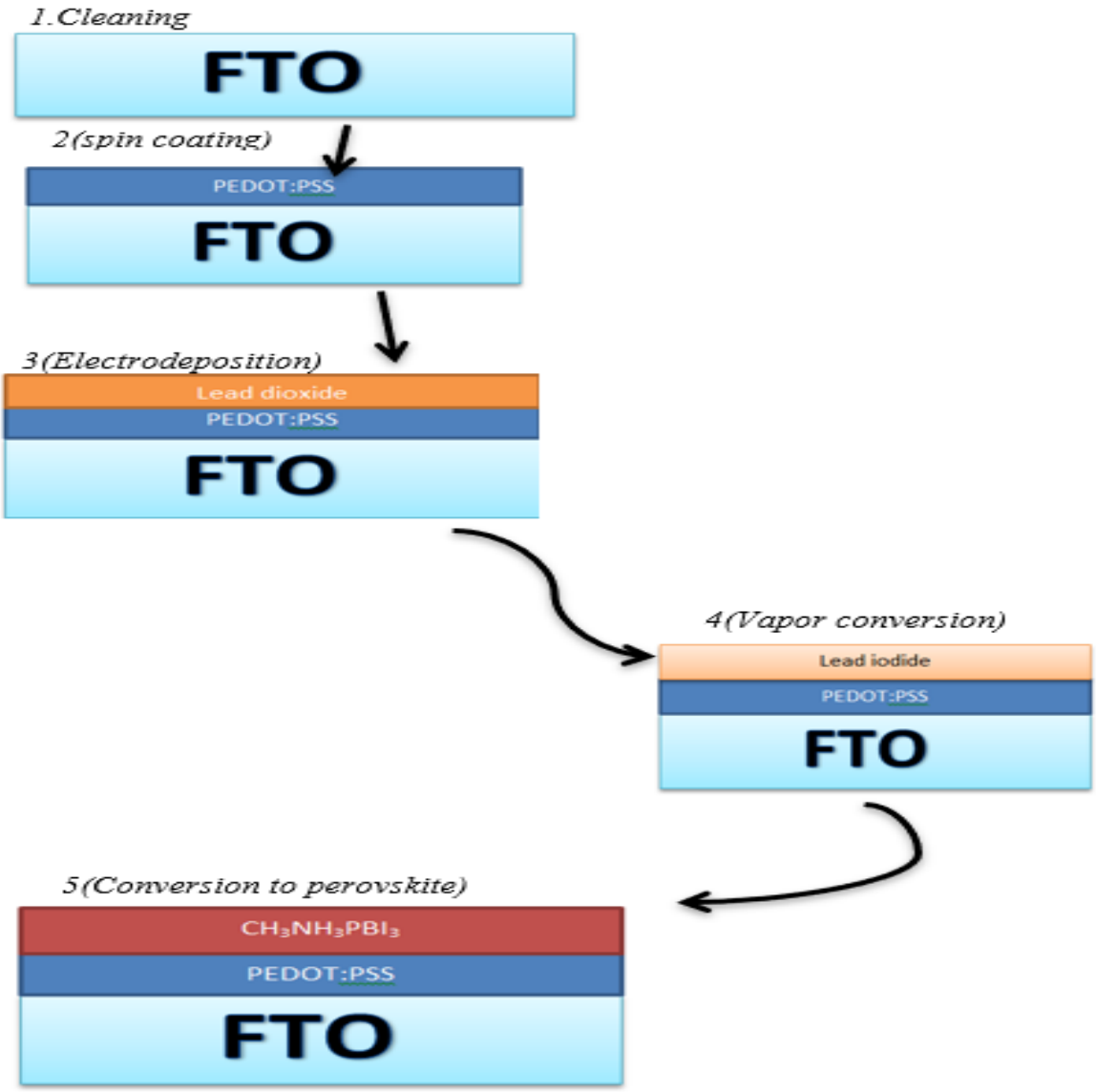

Figure 13: Schematics of electrochemical deposition process including several conversions

After the cleaning process, coating processes were undertaken and each step and the mechanism behind the steps has been explained below. As shown in the figure 13, the first part of the experiment starts with the coating of the absorbing layer of PEDOT:PSS on top of the FTO sample which was followed by the electrochemical deposition of lead dioxide and finally the conversion of lead dioxide to lead iodide .After the conversion of lead dioxide to lead iodide, perovskite formation takes place with the introduction of the sample to the perovskite solution in dark condition for some time period.

2.1.2.1 Fabrication of PEDOT: PSS layer

PEDOT: PSS in the perovskite based solar cell acts as electron transport layer because when a photon hits the light absorbing layer of perovskite the electron emitted from it transfers to this layer whereas hole is established on polymer part of the cell, (PCBM) on usual solar cell. So, fabrication quality and stability of this layer formed eventually will impact the following layers on the cell resulting the performance of final solar cell[34,35].

PEDOT: PSS (poly(3,4-ethylenedioxythiophene) polystyrene sulfonate) was spin coated on cleaned FTO substrate with mechanism of using the centrifugal force to make the coating material on top of the spinning substrate spread all over the surface to from a film. Surface of spin coating was maintained carefully for avoiding any impurities with manual cleaning and the dried sample of FTO glass(2.5cm*2.5cm) was introduced on the coating area and 120µl of warm PEDOT: PSS solution was dropped on the FTO surface with the help of pipette. Since the viscosity of PEDOT: PSS solution is high in low temperature, it is heated resulting in the increase of its viscosity making it convenient for the spin coating process and its uniformity in the layer. PEDOT: PSS solution was taken, warmed up in oven for 30 minutes at 50°C followed by filtering it through disposable CA-CN syringe microporous 0.45µm filter to block particles larger than 0.45µm. The solution was again introduced to oven for 10 minutes more at 50°C. This process was recommended for the uniform solution temperature for spin coating.

After the completion of spin coating process, the sample was put on the vacuum oven at 80 °C for 10 min for uniform layer formation. Since there are many sub-steps involved in the step of spin coating there are different parameters like temperature of PEDOT: PSS solution, volume of solution dropped to the substrate, dropping methods (dynamic, static), spin coating speed, spin time, sintering time, and sintering temperature.

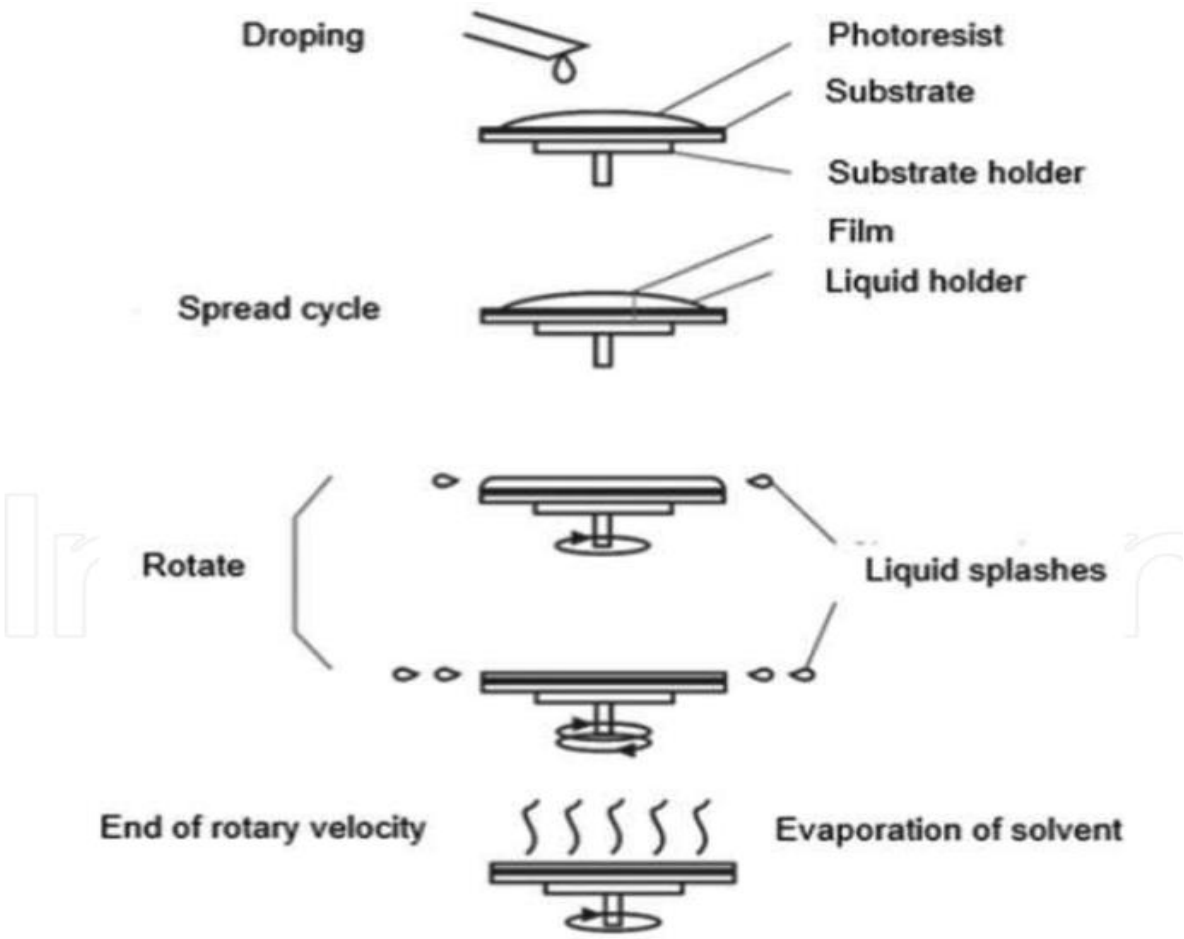

Figure 14: Mechanism of spin coating[36]

2.1.2.2 Lead dioxide deposition

As mentioned on the framework representation on figure 14, formation of perovskite layer involves electrodeposition of lead dioxide on top of PEDOT: PSS followed by conversion to iodide and concluding to perovskite layer. Lead dioxide film quality will determine the conversion to lead iodide and following perovskite formed. For the research 3-electrode system cell was constructed.

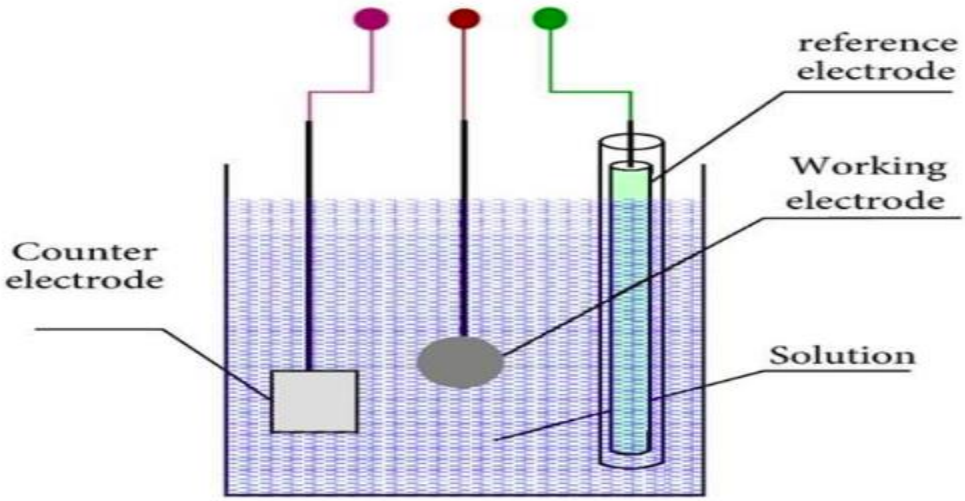

Figure 15: Sketch of electroplating system[37]

The working electrode used is FTO glass with PEDOT: PSS layer on top, reference electrode is Ag/AgCl and the counter electrode is Platinum (Pt). Figure 15 shows the sketch of electroplating system with working electrode, mainly material ranging from inert materials to inert carbon providing the site for the occurrence of reaction. Reference electrode (Ag/AgCl) provides a stable potential during the working process of the system. The potential of working and counter electrodes may change during the reaction happens in the system. In order to detect the precise potential of them, reference electrode is needed. If the potential of counter electrode stays the same or have a rather slight change during the procedure, the reference electrode can be absent from the system. Counter electrode is used in the system to form an electron loop with working electrode in order to make sure the desired reaction can happen at the working electrode while the mechanism of the reaction can also be studied. The material used for counter electrode should have small resistance and the size used is normally 5 times larger than the size of working electrode.

There are two electrical circuits in the 3-electrode system. Working and reference electrode form one circuit to make sure the chemical reaction happens at the working electrode. The main advantage of a three-electrode experiment over a two-electrode experiment is that the results are more stable.

For two electrode system, the counter electrode is theoretically used as reference electrode. The potential of the counter electrode in a cell going through electrochemical reaction is changing all the time. The obtained results, as a consequence, are not stable.

Three electrode potentiostat read the potential difference between the reference electrode and the working electrode using a very small DC current. By comparing the potential measured to the desired voltage level as input using function generator, one can adjust the voltage of the counter electrode until the difference between the desired voltage and the measured voltage is zero. Usual requirements for reference electrode are that it is stable in high temperature and not as poisonous as an also commonly used reference electrode- calomel electrode. In water, AgCl has a low resolvability as 10^{-5} (25°C), while in saturated KCl water solution, it has a resolvability of 10 g/L. Light would accumulate the decomposition of AgCl, it is recommended to keep the electrode away from direct light.

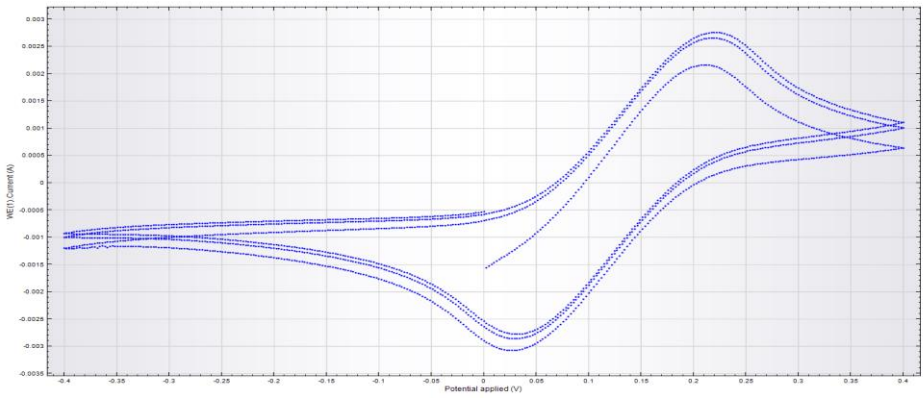

Figure 16: Calibration of Ag/AgCl electrode

Peak position 2: 0.0324V;

peak position 3: 0.2083V $E = \frac{0.2083 - 0.0324}{2} V = 0.08795V$

reference electrode made has a potential of 0.08795V ≈ 0.10 V

Chemistry behind the electrochemistry of lead dioxide deposition is given as:

$Pb^{2+}(l) + 2OH^{-}(l) = PbO_2(s) + 2H_2(g)$

Electrolyte solution was prepared by dissolving 3.7935g of Pb $(CH_3COO)_2$, 1.6998g of $NaNO_3$ and 0.694mL of HNO_3 in deionized water to make a aqueous solution of 100ml solution.

Potentiostat Mode: Cyclic Voltammetry Potentiostatic Mode.

Current range: 10mA-1mA.

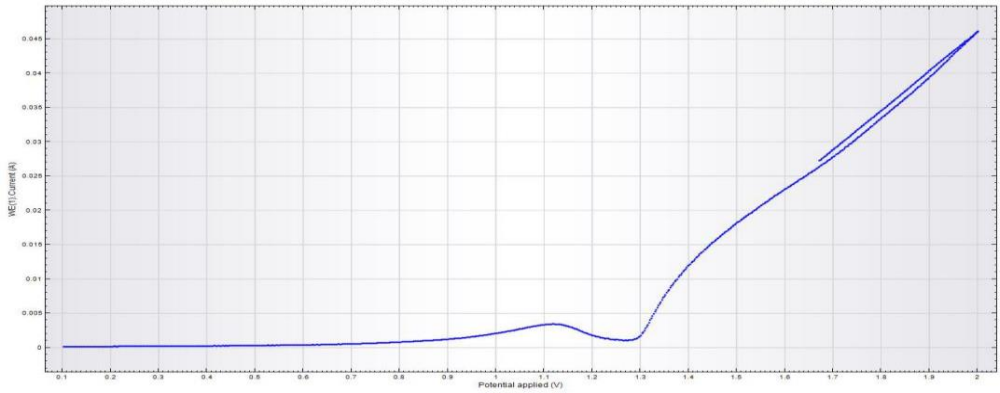

Figure 17: Initiation stage of PbO_2 deposition

From the figure above, it is clear that PbO_2 deposition starts on the PEDOT: PSS when voltage reaches around 1.3V thus the voltage required for the film formation is larger than 1.3V. After several hit and trial method performed in the lab the electrodeposition parameters for lead dioxide was found to be 90 s for 1.3 V.

2.1.2.3 Conversion to Lead Iodide (PbI_2)

During this thesis lead iodide was prepared from the chemical conversion of lead dioxide by dropping the substrate into a container of hydrogen iodide and ethanol and the conversion could be visually seen from the changes in coatings color from light brown to yellow which indicates the conversion of dioxide into iodide. Temperature of the HI solution and the concentration of HI are the main factors that have direct impact on the conversion of lead dioxide into its iodide form.

The fundamental chemical reaction between lead dioxide and hydrogen iodide (HI) (dissolved in ethanol (0.0125M) will result in the lead iodide. The reaction can be deducted as:

$$PbO_2\ (S) + 4HI\ (L) \rightarrow PbI_2(S) + 2H_2O\ (L) + I_2(S)$$

HI solution (0.0125M) was warmed at 60°C hot plate for 3min on a hot bed and then substrate was dipped into warmed solution for 4min resulting in the formation of high-quality film. Visually looks better than last one. 60°C was chosen because the boiling point of ethanol is around 70°C. In 60°C, the reaction of conversion happens faster. The quality of film also increased.

Since, lead iodide is bright yellow odorless hexagonal crystalline solid, boiling point of 954°C which consists of $Pb^{2+}$and I^{-}salts usually resembling small hexagonal platelets, giving the yellow precipitate a silky appearance whereas larger crystals can be obtained by exploiting the fact that solubility of lead iodide in water increases dramatically with temperature [2]. The compound is colorless when dissolved in hot water, but crystallizes on cooling as thin but visibly larger bright yellow flakes, that settle slowly through the liquid giving a visual effect often described as "golden rain"[38].

2.1.2.4 Perovskite Layer conversion

After obtaining lead iodide layer, it is converted to perovskite by chemical reaction with methyl ammonium iodide (MAI). The substrate covered by lead iodide was submerged in a solution of MAI isopropanol of concentration of 10mg/mL under dark condition for 2 hours.
Preparation of perovskite can be noticed after the formation of brownish film on top of lead iodide.

$$PbI_2 + CH_3NH_3I \rightarrow CH_3NH_3PbI_3 \text{(Methyl Ammonium Lead Iodide) (Perovskite)}$$

2.1.3 *Ultrasonic spray coating*

Spraying technology is commonly used method to produce smooth and uniform layers, with benefits like its affordability and suitability for large-scale manufacturing, manufacturing efficiency, efficient use of starting materials and good control of coating. The advantage of ultrasonic vaporization for normal airborne atomizing is that, that in the ultrasound spray the size of droplets of fog and the density of the fog can be achieved independently of each other. In spray air, spray drops size can be reduced only at the expense of fog density due to droplets to increase the air flow rate. Other benefits independently in addition to the variable process parameters that are smaller; the size distribution of the droplets is good repeatability, wide range of different and different nozzles as well as equipment good operational reliability.

Ultrasonic diffusion is based on piezoelectric elements that are oscillated at a high frequency (20 kHz-3 MHz). Piezoelectric material is a material that can be electrically polarized if subjected to mechanical stress. Similarly, in an external electric field, the piezoelectric material can be modified shape and vibrate. Vibration of piezoelectric components is obtained in the nozzle through which the liquid flows, to vibrate, whereby the ultrasonic vibration passes and causes the formation of droplets[39].

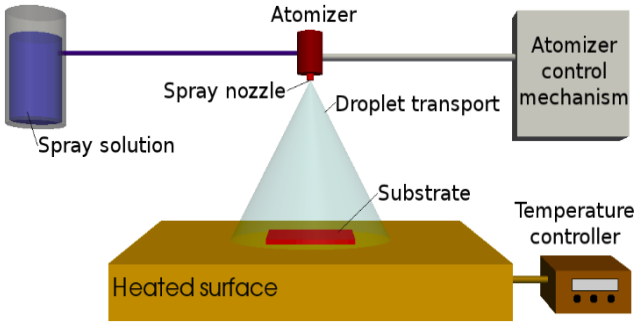

Figure 18: Schematics of Ultrasonic spray coating [20]

The drop-in liquid by the effect of ultrasound is based on two phenomena that are formation of capillary waves and cavitation. Capillary waves are standing wave motion that occurs when the liquid surface vibrates perpendicularly to the ultrasonic frequencies against the oscillating surface. The sound waves generated by the oscillating surface are transmitted through the liquid and cause the surface to oscillate. When the vibration increases enough large capillary wave's amplitude increases so that the liquid begins to drop from the top of the capillary waves. When the liquid's drizzling starts, then the amplitude of the capillary waves no longer increases and all ultrasound energy consumes fluid entrain[39].

Another important factor was cavitation. Cavitation is the gas bubbles in the liquid birth, growth and impliosis. When the sound waves pass through the liquid, they make up alternating denser and fewer areas just like the sound waves in the air. At the lower pressure stage, bubbles may form, which may expand, resulting in pressure within them falls. At a higher-pressure stage, the pressure may cause a bubble emplacement, whereby the pressure inside the bubble may be many times greater than without the air pressure. From this sudden bubbling of bubbles follows the hydraulic shock wave resulting in the formation of droplets on the surface of the liquid. However, the frequency of cavitation bubbles is low, so they are less dependent upon the frequencies used.

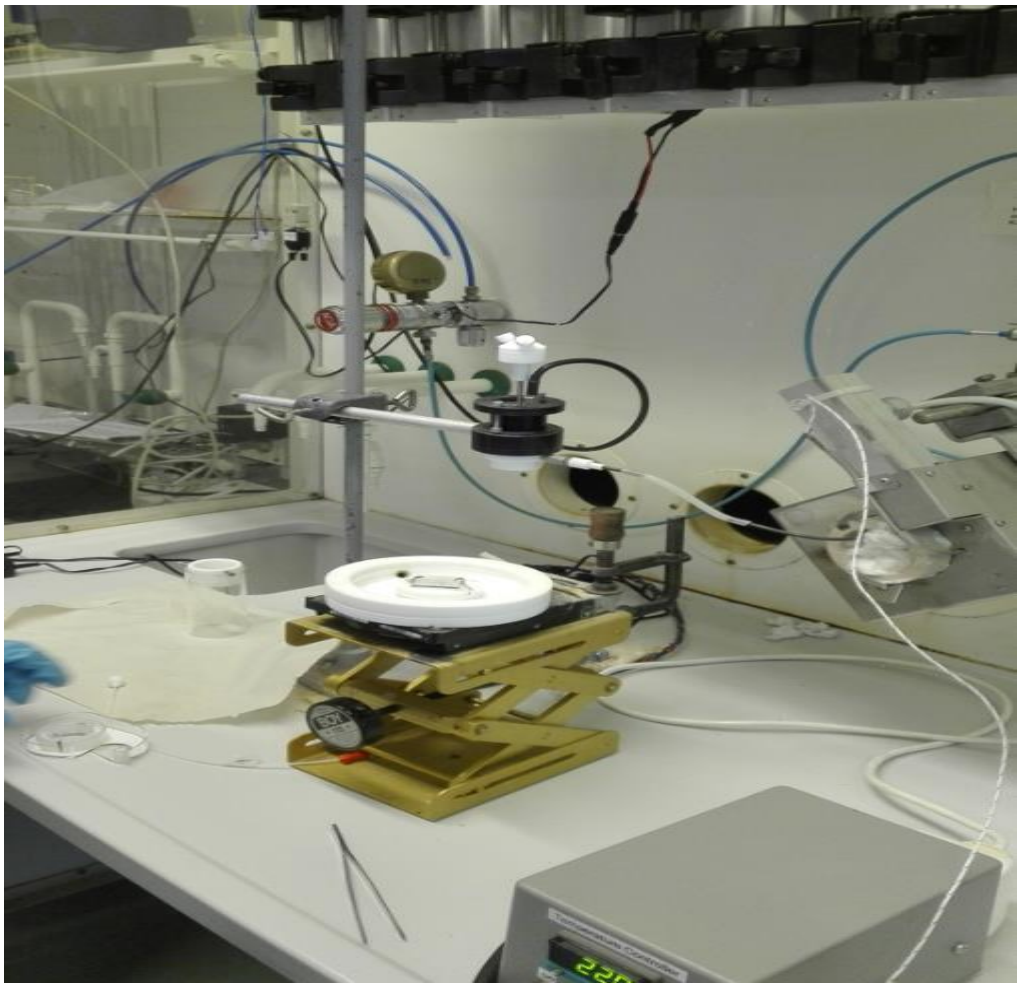

Figure 19: Ultrasonic spray coating utilities laboratory Turku university (2018)

2.1.4 *Dip coating*

Dip coating is the process where a substrate is immersed into a container of solution (coating material), removed from it and allowing it to drain. For this thesis, the experimental step for dip coating started as the substrates were baked at 80 ºC for 10 min in normal oven and then the substrates were immersed (dip coated) in perovskite solution for a moment (1 sec). The coating procedure was followed by annealing of the substrate in vacuum oven for 20 min at 80 ºC.

Dip coating process involves basically three steps

1. Immersion: immersed in perovskite solution manually at constant speed
2. Dwell time: a moment (1 sec)
3. Withdrawal: the substrate was withdrawn manually at constant speed to avoid judders. Faster the substrate is withdrawn, thicker will be the coatings on the substrate[40].

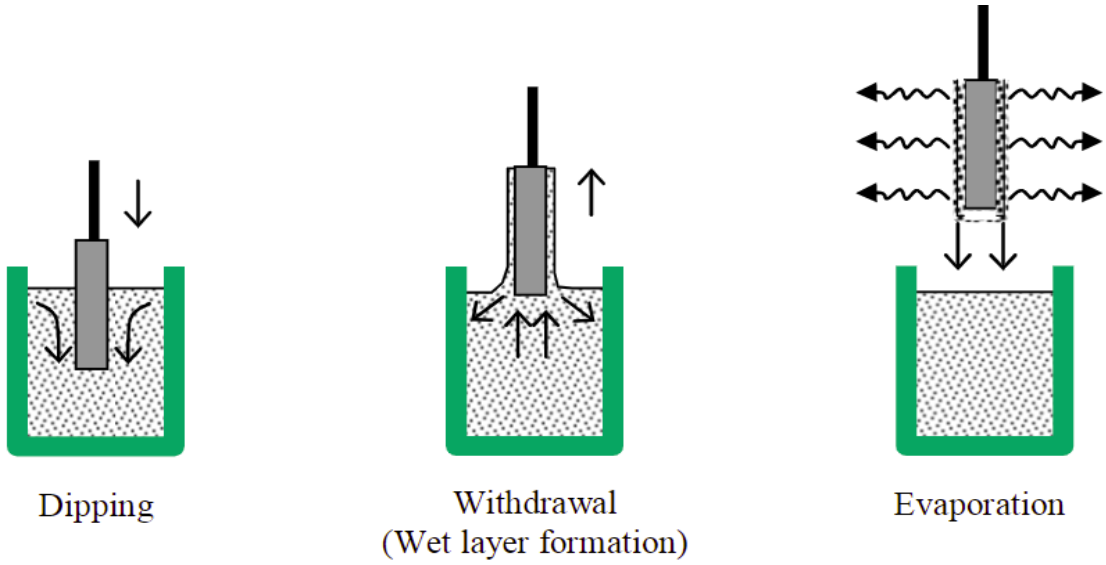

Figure 20: Schematics and mechanism behind dip coating[40]

2.2 Degradation process

Stability of perovskite layer (absorbing layer) has been a hindering factor for the perovskite solar cell for commercial production and use. In lab, after few hours today's exposure to normal room condition of temperature and humidity, the degradation of perovskite could be easily noticed from the change of color of the coating from brownish red to yellowish. Perovskite is thought to be unstable because of its low crystal formation energy and hydroscopic nature[41,42].

2.3 Protection by Polymer layer (PMMA)

The main factor for the current photovoltaics other than power conversion efficiency (PCE) are its stability, its fabrication cost and the cost of processing. The issues of degradation and stability of the device using perovskite should be addressed to achieve good reproducibility and the longer stability. In this thesis, degradation mechanism was studied and a direct exposure to ambient temperature and moisture was disabled with the use of layer which would not have a similar impact on the surface degradation than the hybrid perovskites. Since the polymer layer on the top of perovskite would be beneficial to avoid the direct perovskite- moisture exposure[14,43].

For the preparation of polymer layer that protects the perovskite for accelerated degradation, PMMA solution was prepared and for the preparation of the solution, PMMA granules were taken and dissolved in 100 ml of chlorobenzene.

The amount of PMMA needed for the solution of PMMA was calculated from

W = PX/100 – P

Where P is concentration in percent (w/w).

X is weight of the solvent

W is weight of PMMA

For sample size, PMMA solution weighing 70 mg was dissolved in around 1 mL chlorobenzene in Eppendorf tubes.

The solution was mixed with the help of magnetic stirrer. Some water was added into the jacket to couple heat from the jacket to the bottle. PMMA solution thus obtained was coated on the sample using Spin coating method and the spin coater parameter was found out to be 3000 rpm for 15 seconds. After the completion of spin coating process coated sample was placed inside an oven with temperature of 80 ^{o}C for 10 min and finally the sample was removed from the oven and let it cooled down then prepare for surface characterization[44,45].

3. Results and Discussion

3.1 Perovskite Formation

3.1.1 *Spin coating*

Spin coating was performed in the lab using perovskite solution and spin coating parameters as mentioned in the experimental part and after the completion of spin coating followed by its introduction to vacuum oven. Later, the surface was studied with the help of Raman microscopy and some microscopic studies of surface morphology was done and explained below:

Figure 21: Spin coated perovskite on top of FTO substrate after annealing process

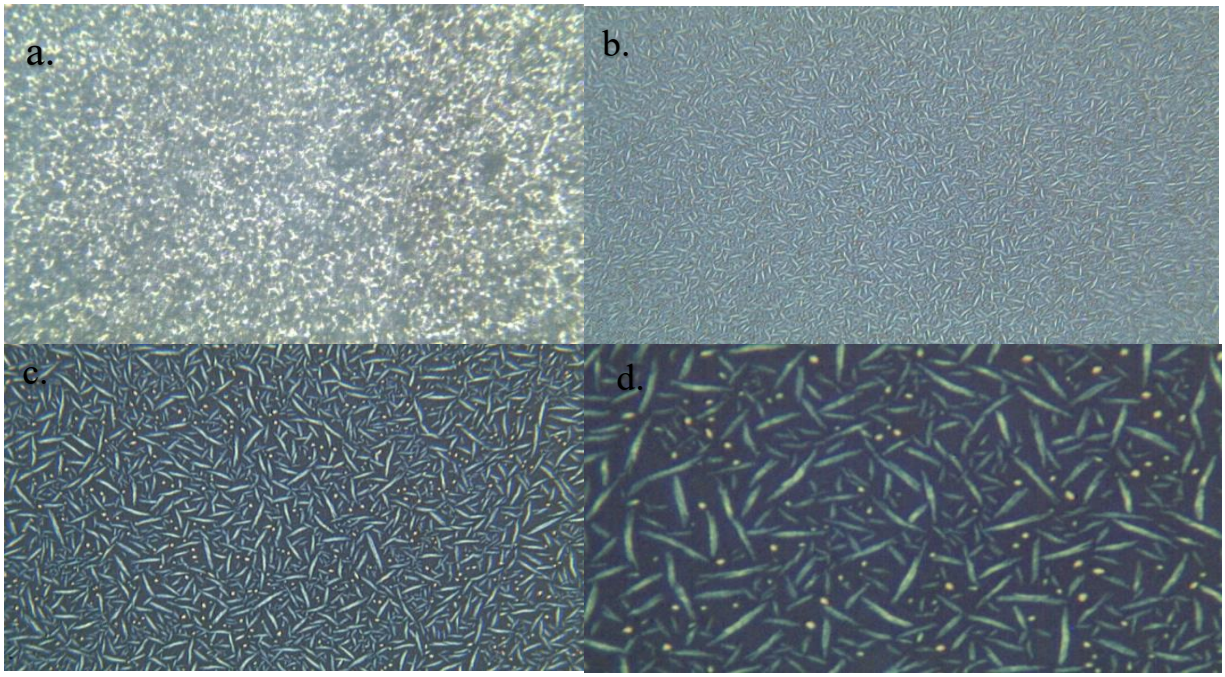

Figure 22: Raman microscopic image of spin coated perovskite (a) 5x; (b)20 x; (c)50 x and (d) 100x magnification

Conveniences of spin coating are as follows:

- Easy and fast operation
- Easy to change parameters for changing film thickness
- If correct parameter, uniform film thickness
- Absence of coupled process variables

However, finding an ideal parameter for obtaining uniform thickness of perovskite layer is a difficult task and if not, then there are some defects which could be seen during microscopic studies as shown in figure (23):

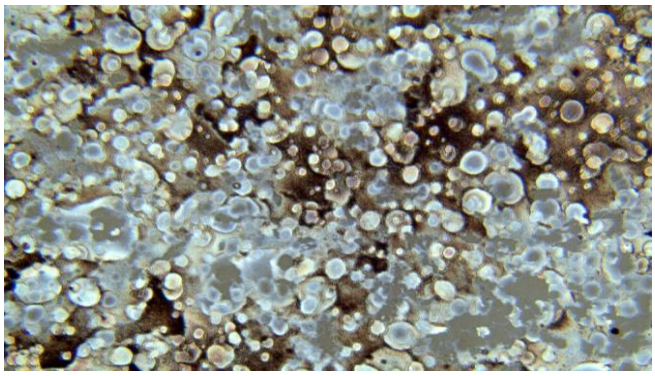

Figure 23: Raman microscopic image 5x of unsuccessful spin coating (bubbles)

Along with the bubbles there are other defects in the process which could be hindering the formation of ideal perovskite layer. Some of the defects are as:

- Swirling pattern
- Chuck mark
- Uncoated area substrate
- Pin hole defect

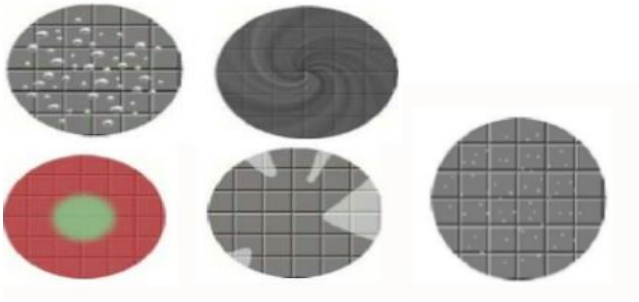

Figure 24: common defects during spin coating schematics[46]

Along with these defects, some inconveniences while using the process are its difficulty to implement on large substrate as many parameters are affecting the final result and wastage of coating material during the process doesn't help the material efficiency[30].

3.1.2 Electrochemical deposition

During the electrochemical deposition process, first the samples were cleaned and sanitized using plasma cleaner. For this process, PEDOT: PSS was coated as hole transport layer followed by electrodeposition of lead dioxide and its conversion to lead iodide. Finally, experiments were conducted for the conversion of lead iodide film into perovskite and results were obtained for further evaluation.

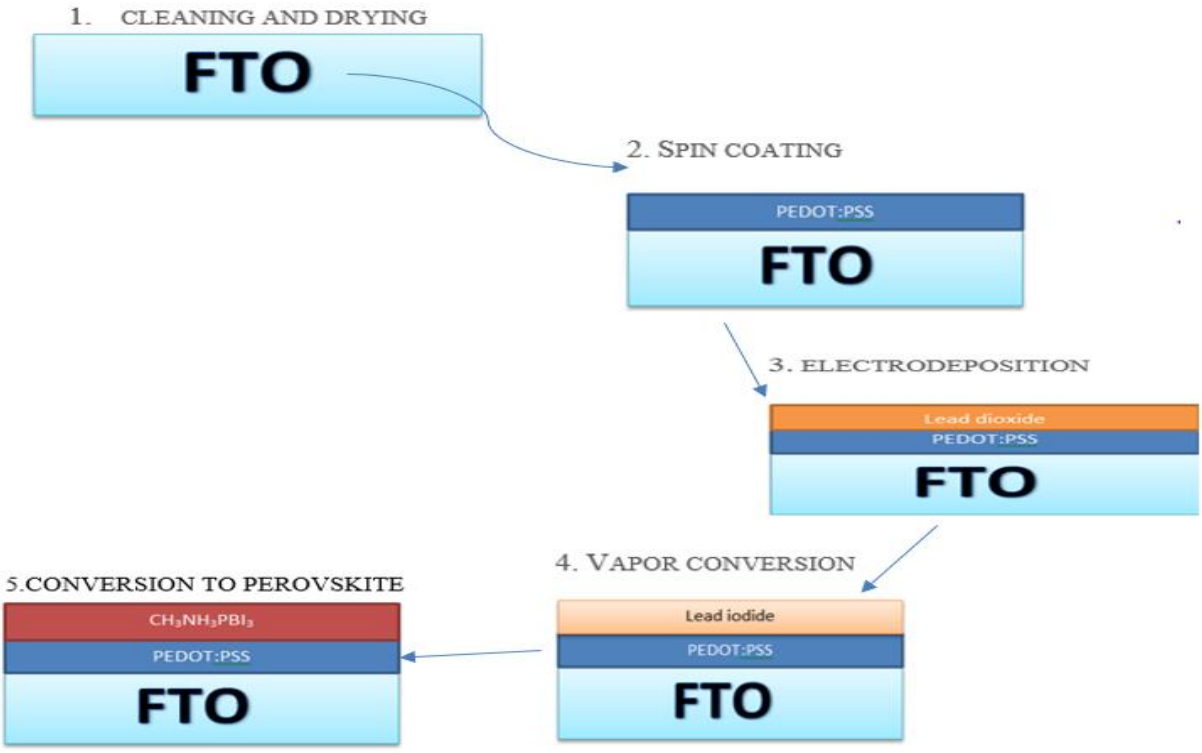

Figure 25: Schematics of electrochemical deposition process including several conversions

3.1.2.1 Spin coating of PEDOT: PSS

A hole transport layer (HTL) plays a key role in efficient hole extraction and transfer in inverted planar perovskite solar cells. A 10–20 nm thick poly (3,4-ethylenedioxythiphene): poly(styrenesulfonate) (PEDOT: PSS) layer is the most popular HTL in such a device structure. PEDOT: PSS was warmed at 50℃ for 30 min and filtered through 1.55 mm filter followed by warming the PEDOT: PSS at 50℃ in oven for 10 min. After this process, the solution is ready for spin coating and for thesis it was spin speed of 1000 rpm for 60s. (50 µL of 50℃).
After the coating, the substrate is put into an oven of 110℃ and sintered for 15min (After the coating, the substrate is put into a vacuum oven at 80℃ and sintered for 15 min).

Centrifugal force is the main mechanism of spin coating technique. Thus, it is obvious to relate the speed of rotation and the volume used to the final performance of product. With fixed conditions, relationship among products quality, speed of spin and volume used were discussed. In order to study the influence of time in oven, time for spin coating, volume and whether dynamic method as well as static method influences the performance of sample when other parameters changes[17,30].

Since the spin coating was performed with ambient parameters of temperature and pressure so the results are not controlled with precision because of the uncontrolled temperature of solution and the ways to operate dynamic spin coating. Also, from UV- vis spectra, one can realize that the thickness of the central part of sample is different from it of the edge part. Central part is thicker than edge part and samples were introduced to the Raman spectroscopy. After the clearance of dark spots and background from the Raman spectra, it shows strong signals of PEDOT:PSS around 1436cm^{-1} which was identical to the theoretical one as shown in figure 26[47].

As found from the experiment the optimized combination of parameters for PEDOT: PSS spin coat is 1500rpm, 30s, PEDOT: PSS, 120µL (50°C), 80°C on vacuum oven for 15 min.

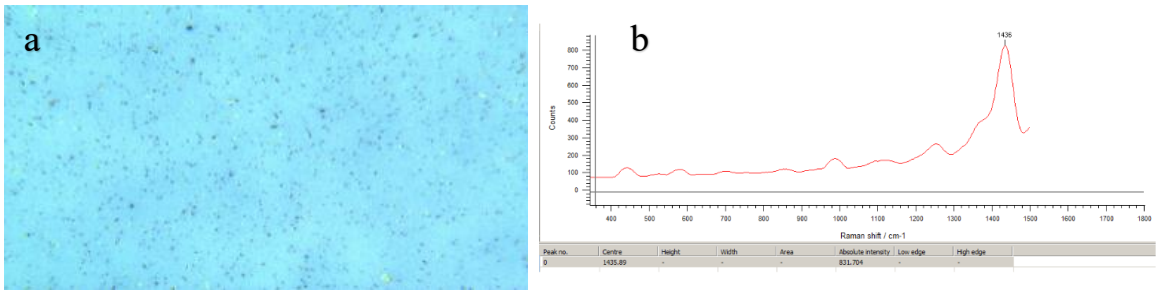

Figure 26: (a) Raman microscopic image of PEDOT: PSS coatings; (b) Raman spectroscopic image with Raman peak at 1436 cm-1 showing similarities with theoretical findings [47].

3.1.2.2 Electroplating of Lead Dioxide

Electrolyte for deposition was prepared by mixing 3.7935g of Pb $(CH_3COO)_2$, 1.6998g of $NaNO_3$ and 0.694mL of HNO_3 in deionized water to make a 100ml solution. Lead dioxide was deposited onto FTO/PEDOT: PSS film with deposition time of is 90 for 1.3 V and to have a better understanding of the electroplating process, one need to know the initiation point for PbO_2 electrodeposition.

Reaction: $\boldsymbol{Pb^{2+}(l) + 2OH^{-}(l) \text{-----} PbO_2(s) + 2H_2(g)}$

Potentiostat Mode: cyclic voltammetry potentiostat mode.

Current range: 10mA-1mA.

The solution for deposition needs to be paid attention to and kept away from air, to avoid the contamination found in samples. Theoretically, the solution can be used for many times because the concentration of Pb^{2+} is much more than needed. However, the working electrode used is 2.5cm*2.5cm FTO glass, which have a rather large area.

In this case, solution needs to be replaced after few depositions to maintain the required concentration of the electrolyte for better result.

In the experiments, the counter electrode is made of Pt cylindrical mesh. Theoretically, it would be good for counter electrodes to have high surface area. The counter electrode made of platinum cylinder is more ideal than the counter electrode made of Pt mesh and wire because of its higher surface area as both electrodes were both tested in this experiment concluding that Pt cylinder gives better performance (coverage and thickness) than the other one[18,33].

Figure 27: Electrochemical cell Turku university

After the procedure the cell was set as FTO glass as working electrode, Ag/AgCl as reference electrode and Pt as counter electrode. Cyclic voltammetry potentiostatic mode in potentiostat is used in this calibration.

In the experiments, it was also been found that the lead dioxide film is highly sensitive. Even a slight contact may leave a severe scratch. After deposition, the working electrode needs to be flushed with deionized water for cleaning. Before the conversion into PbI_2, the samples need to be carefully stored. Three different methods of storage were utilized in this part: put samples in open environment; stored in Ethanol; stored in deionized water. Ethanol and deionized water were chosen because none of them can dissolve lead dioxide. Samples put in open surrounding shows the worst appearance. Many lines and scratches can be found. Samples stored in Ethanol and deionized water shows similar results and barely any damage can be found. Ethanol was finally determined to be the storage solution at last. It is highly volatile, so it can save much time when dry lead dioxide samples are needed.

Detailed parameters used are shown below.

Start potential	0V
Upper vertex potential	0.4V
Lower vertex potential	-0.4V
Stop potential	0V
Number of crossing	6
Highest current range	1mA
Lowest current range	100μA

The vertex potential range and current potential range were studied to get the best results. Before the measurement, background of the electrolyte needs to be tested to make sure no peak of solvent shows in the vertex range used. In this case, deionized water is the background. When scan of deionized water in the potential range of -0.4V to 0.4V shows no peak in the range used then the electrolyte is considered to be ideal to use.

Theoretically, the reference electrode needed to be calibrated before and after every electroplating procedure. It is a tedious work and time-consuming procedure[48]. In the experiments of this report, it has been tested over 100 times that the reference electrode is stable.

The potential of the reference electrode remains around 0.09V before and after each experiment. Some value shifts can be seen when testing the reference value at different measurements. That is due to the electrode position change in different measures. The potential value difference is less than 0.1V which is a small value comparing to the voltage used (around 1.3V). In order to save time, calibrate once and the electrode can be used to deposit 5 times.

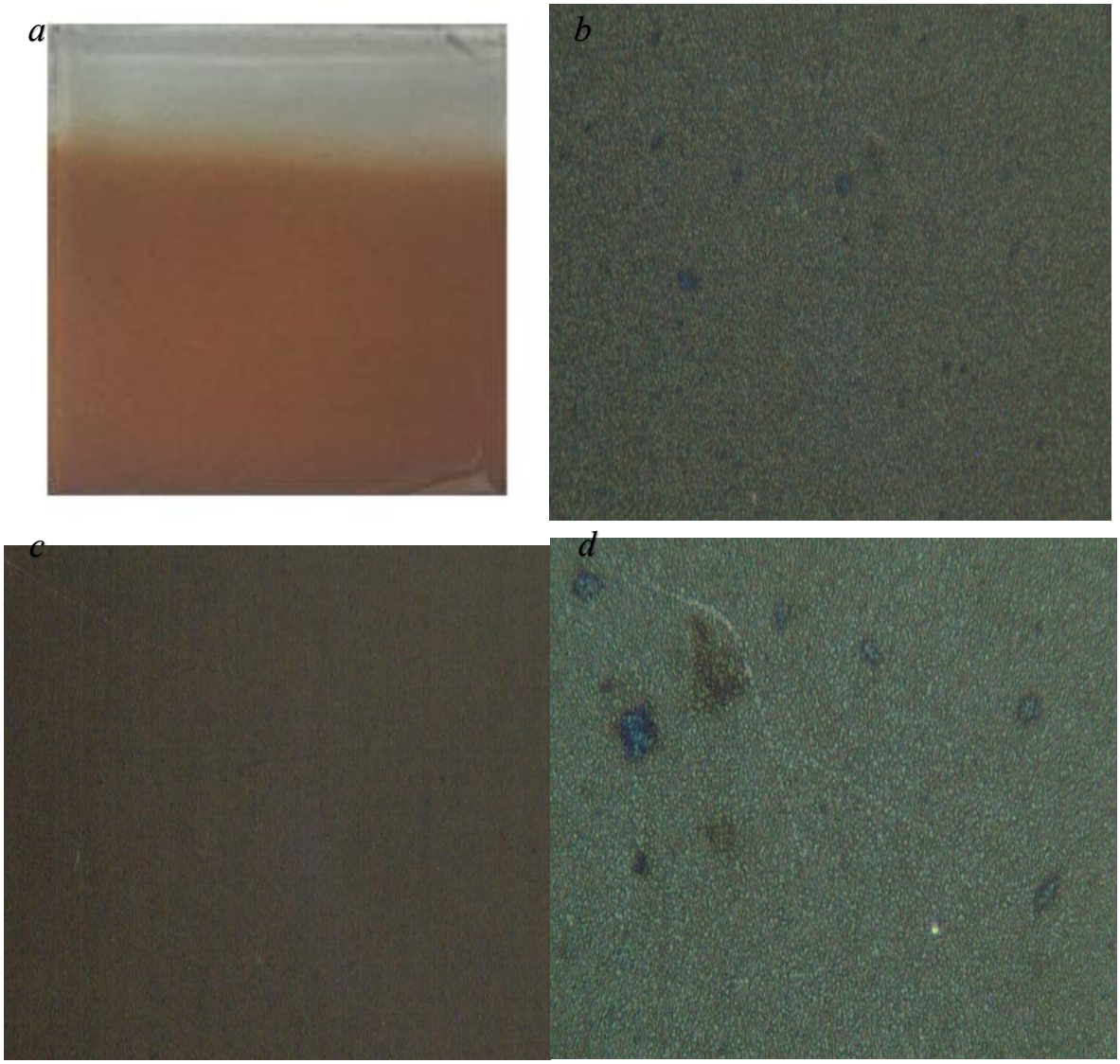

Figure 28: (a) General picture of PbO_2 in lab and Raman microscopic image of PbO_2 on PEDOT: PSS (b)5x ;(c)20x ;(d)50x

3.1.2.3 Lead Iodide Conversion

Many approaches can be used to convert lead dioxide to lead iodide. Basically, every approach follows the fundamental chemical reaction between lead dioxide and hydrogen iodide (HI). HI was dissolved in ethanol (0.0125M). The reaction can be deducted as:

$$PbO_2\,(S) + 4HI(L) \rightarrow PbI_2(S) + 2H_2O(L) + I_2(S)$$

The overall idea is to submerge the samples into HI solution. The experiment cannot be easily controlled because the high acidity of HI. Appearance of yellowish color on top of lead dioxide concludes the conversion of lead dioxide into lead iodide. The crucial part of this method is adjusting the concentration and time of conversion for the formation of film to be even and

homogeneous.

Too concentrated solution can convert the film in a very short time and cannot be precisely controlled. On the other hand, if the concentration is much too low, the conversion can be a long progress.

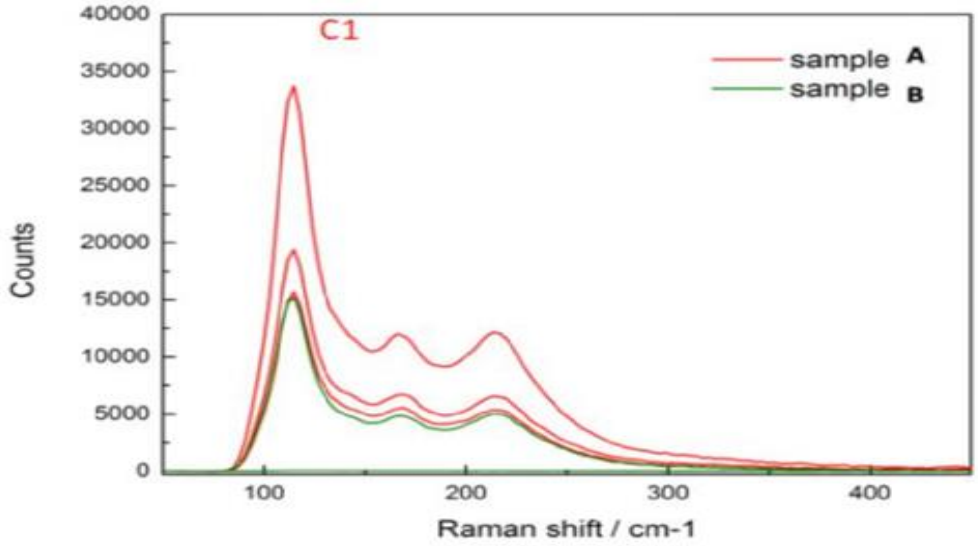

Figure 29: Raman spectra of PbI_2 thin films with excitation at 532 nm with strong signals around 100-120cm^{-1}

The appearances of PbI_2 can be confirmed using Raman spectroscopy as the signals from lead iodide can be seen in the range less than 100-120 cm^{-1}, which is beyond the range of the Raman system owned by the research lab. Hence, IR spectroscopy could be an effective tool to prove the existence of lead iodide.

It can be seen from the curves that spectra gathered at 70°C shows the highest absorbance of all spectra gathered. As for the background, PEDOT: PSS shows more clear results than FTO glass. Thus, it was concluded that 70°C and PEDOT: PSS background is most ideal for the IR experiments of PbO_2.The amount of scan is 62 and the resolution is 4 cm^{-1}. The IR peak of PEDOT: PSS is around 1094 cm^{-1}. The signal is not strong enough to be sure that around 500 cm^{-1} exists signals for lead dioxide.

Samples put in open surrounding shows the worst appearance. Many lines and scratches can be found. Samples stored in Ethanol and deionized water shows similar results--barely any damage could be found. Ethanol was finally determined to be the storage solution at last. It is highly volatile, so it can save much time when dry lead dioxide samples are needed.

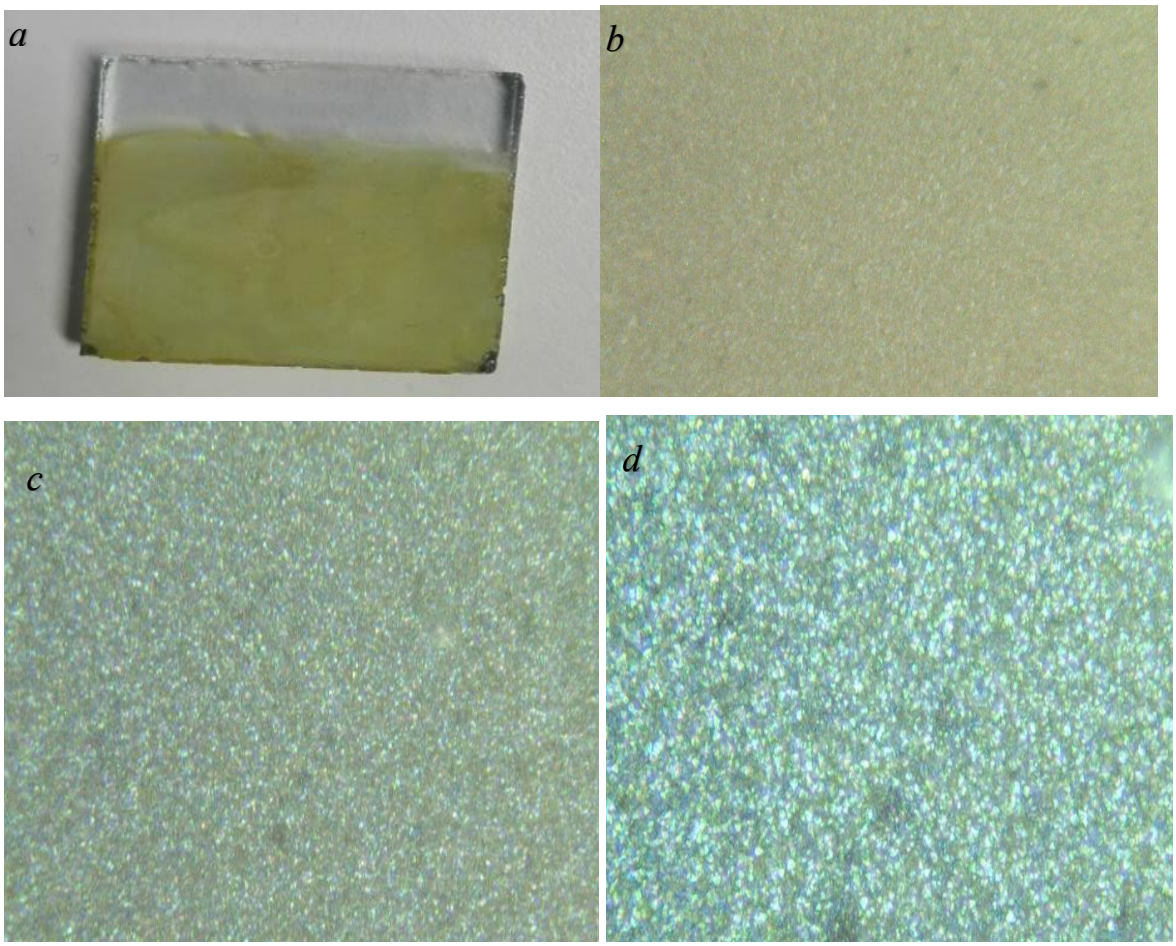

Figure 30: PbI_2 layer on FTO Microscope images (x50) of PbI_2 layer on top of PEDOT: PSS and Raman spectroscopy image. A) Microscope image sample A; B) Microscope image of sample B; C1) and C2) Raman images in different ranges

3.1.3 *Ultrasonic spray coating*

There are several different parameters for ultrasonic diffusion, which can affect the characteristics of the resulting layer. Such parameters include, for example, liquid flow rate , the size of droplets , the precursor solution concentration , surrounding conditions (humidity, temperature), distance between nozzle and substrate, the use of auxiliary gases , ultrasound frequency, vibration amplitude, voltage used , the substrate temperature and the solvent used and its polarity .The properties of the liquid used with viscosity and surface tension are of great importance in the formation of droplets as they depict the forces that oppose droplet formation. The smaller the surface tension, the smaller the droplets and lower the viscosity, the faster the formation of droplets is. In the ultrasonication, the size of droplets also depends on the vibration frequency as well as the flow rate of the solution. The vibration frequency is inversely proportional to droplets the size of the droplets decreases as the vibration frequency increases.

Also, in addition to the properties of liquid, the fluid temperature and pressure also influences the spraying, as these properties affect the passage of waves in liquid and, therefore affecting the spraying impact. In the preparation of perovskite, the boiling point of the solvent has an effect on the formation of perovskite. If the boiling point of the solvent is too low, the solvent may evaporate before droplets hit the substrate, resulting in loosening of the gaps in the perovskite layer. If, however, the boiling point of the solvent is too high, this will result in the formation layer again, which in turn leads to an uneven surface formation.
The formation of perovskite layer on top of FTO was prepared on the solvent based method from perovskite solution which was prepared from $CH_3NH_3PbI_3$ using either DMF (~ 153 °C) or DMSO (~ 189 °C). The concentration of the precursor solution used was 10 mM.

The formation of a perovskite layer can also be influenced, among other things, by a nozzle and the substrate spraying speed and a precursor solution concentration. Studies have shown that lower the precursor solution concentration lower is the uniformity of the as it's hard to perovskite layer completely cover the surface due to the presence of plenty of holes in it. In addition, a low precursor solution concentration increases heat loss from the surface of the substrate, further aggravating the solvent evaporation from the substrate and harming the crystallization. On the other hand, concentration increasing the viscosity of the precursor solution, which also affects the spreading of the solution on the surface of the substrate. Thus, finding the correct perovskite solution concentration is a must for good perovskite layers manufacturing. There have been many studies have explained how the precursor solution concentration affects perovskite layer formation. As a solvent, DMF was used with methyl ammonium lead iodide ($CH_3NH_3PbI_3$) to prepare perovskite solution[11,39].

The advantage of ultrasonic vaporization for normal airborne atomizing is that, that in the ultrasound spray the size of droplets of fog and the density of the fog can be achieved independently of each other. In spray air, spray drops size can be reduced only at the expense of fog density due to droplets to increase the air flow rate. Other benefits independently in addition to the variable process parameters that are smaller, the size distribution of the droplets is good repeatability, wide range of nozzles with several diameters and also the flexibility of changing the distance between nozzle and the substrate[49,50].

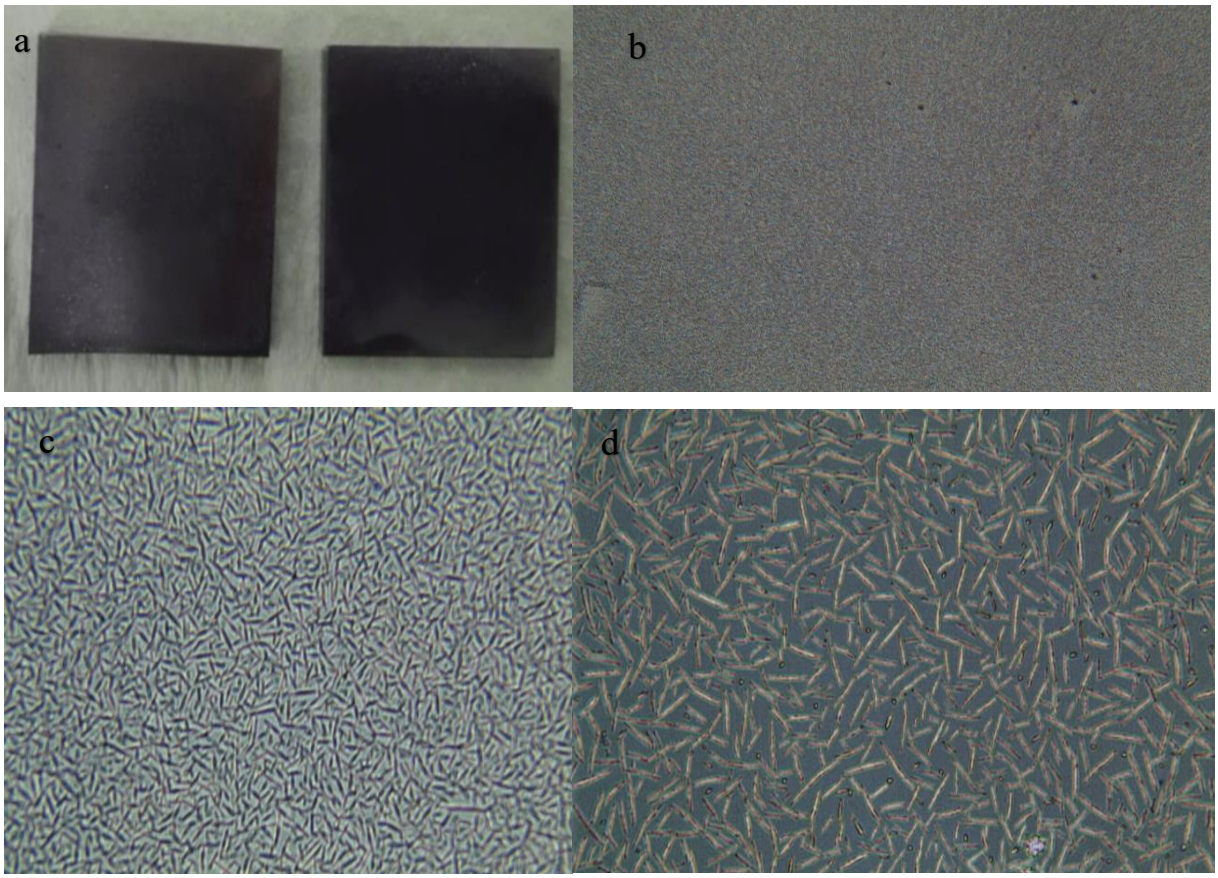

Figure 31: Ultrasonic spray coated perovskite (a) sample picture in lab; Raman microscope images;(b) 5x;(c) 20x;(d)50x magnification

After the preparation of perovskite solution, ultrasonic spray coating was performed, samples were taken for annealing in vacuum oven for 30 min at 90°C.

3.1.4 *Dip coating*

After the formation of perovskite layer after dipping and the annealing process the samples were introduced for further studies with the help of Raman microscopy. One of the advantages of dip coating is its simplicity to perform as any type of beakers or containers can be used to accommodate the shapes of the substrate. However, the drawbacks of manual dipping as performed on lab is its complications to control the thickness uniformity and also the thickness. But the experiment cannot be easily controlled because of the high complexity to controlled dipping factors since the dipping was carried out manually. Since time factor is sensitive to the dipping method success the film would be losing its thickness. The crucial part of this method is adjusting the concentration and time of conversion. From the hit and trial methods used, time for dipping method was found to be 1 second as time is inversely proportional to the thickness obtained.

The coated substrate was then introduced to vacuum oven for annealing process at 80 °C for 20 minutes to obtain optimum quality of perovskite layer on FTO substrate in the lab. Since the manual dipping process is really hard to control obtaining a good quality of perovskite was challenging. Figure 32 (a) shows the general picture taken in lab where figure 32 (b),(c) and (d) shows the spectroscopic image of dip coated perovskite.

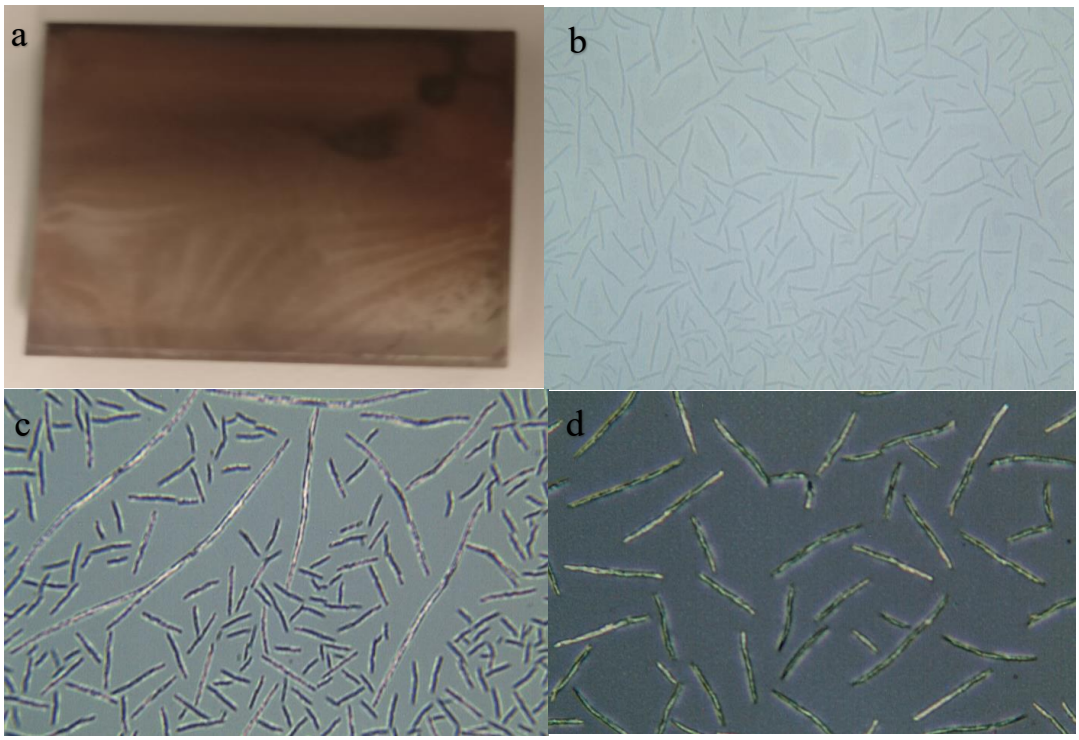

Figure 32: Dip coated perovskite (a) sample picture in lab; Raman Microscope images;(b) 5x;(c) 20x;(d)50x resolution

3.2 Perovskite degradation

The studies performed identifies oxygen, moisture, UV light, solution processing and thermal effects as the main factors behind the degradation of perovskite and the reaction initiated during the process of degradation has been stated below [2,51]. The theoretical background behind the degradation is

$$4MAPI + 8H_2O \rightarrow (CH_3NH_3)_4PbI_6 \cdot 2H_2O + 3Pb(OH)_2 + 6HI \uparrow \quad \textbf{(1)}$$

$$(CH_3NH_3)_4PbI_6 \cdot 2H_2O \rightarrow (CH_3NH_3)_x PbI_{2+x} + (4-x)\, CH_3NH_2 \uparrow + (4-x)\, HI + 2H_2O \quad \textbf{(2)}$$

$$2\,(CH_3NH_3)_x PbI_{2+x} + 2CO_2 + O_2 \rightarrow PbCO3 + 2I_2 \uparrow + 2x\, CH_3NH_2 \uparrow 2xHI \uparrow \quad \textbf{(3)}$$

$$2\,(CH_3NH_3)_x PbI_{2+x} + H_2O + 1/2\, O_2 \rightarrow Pb(OH)_2 + I_2 \uparrow + xHI \uparrow + xCH_3NH_2 \uparrow \quad \textbf{(4)}$$

$$Pb(OH)_2 \rightarrow PbO + H_2O \quad \textbf{(5)}$$

These processes are mainly about the transformation of low band gap MAPI to relatively high band gap hydrate materials. Exposing to light might accelerate the decomposing process. Equation (1) is the hydration process of MAPI and equation (2) is the dehydration of the product of equation (1). Transient phase product (PbI_{2+x}) x- is generated because the hydrate product is only stable in an environment highly humid. That means in ambient conditions, $(CH_3NH_3)_4PbI_6 .2H_2O$ is not stable and can easily react[42]. Following equation (3) to equation (5), MAPI would finally degenerate to form other lead products. This degradation procedure is followed by a color change from black to transparent owing to the formation of hydrated perovskite phases.

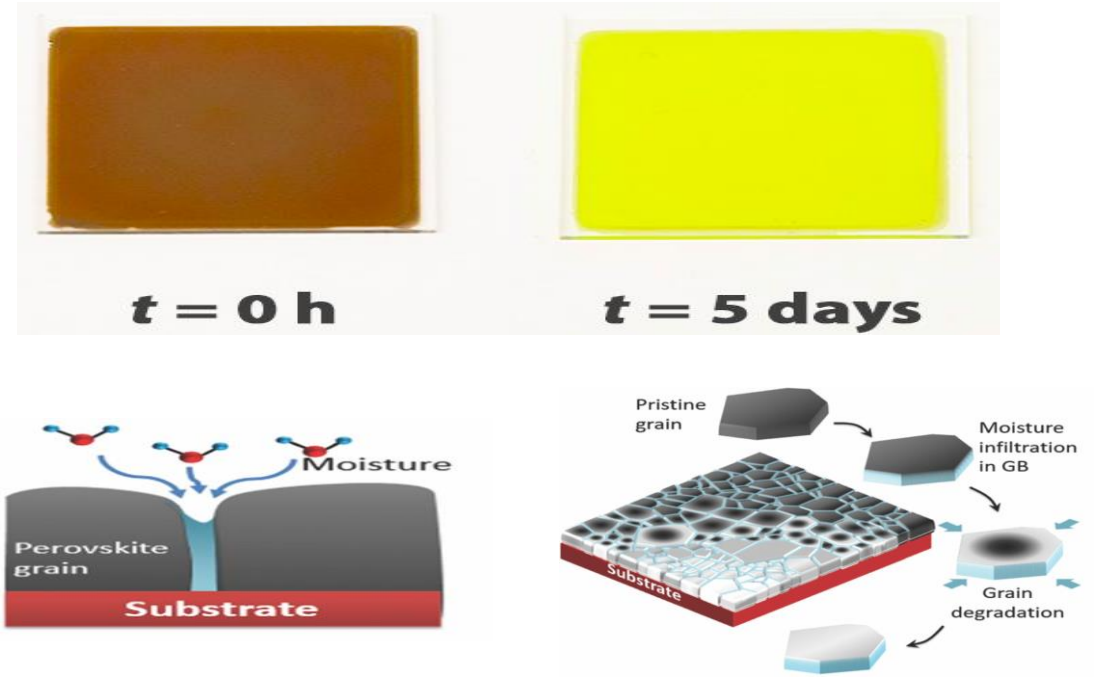

Figure 33: Illustration of how perovskite decompose, GB is short for grain boundaries[52]

Sintering for different time after the formation of perovskite films can provide various grain sizes. During the process, many water sensitive $CH_3NH_2^+$ ions on surface of crystal grains can be eliminated. Principally, larger grain size makes it more durable to humid. For second approach, an example had been given in 1.2.1 Structure of Perovskite. By adjusting the X atoms in ABX_3 structure, the efficiency can be tuned.

It is also reported that MAPI is more sensitive to moisture than $MAPbBr_3$. A atoms are also changed in different ways to test the outcomes of perovskite[53].

The last manipulation is based on the face that most of the methods for perovskite films today, are solvent involved. The reaction of perovskite forming almost always happens in a solution condition. Using a solvent which might react in the procedure, of course, increase the complexity of the experiment, but also gives more possibility to enhance the procedure of perovskite film formation by interact with the reactants. DMSO, DMF, and GBL are common solvent in perovskite film formation, they are active as coordinating ligands that influence the solution chemistry and the behaviors of films. The character of perovskite can also be tuned and influenced by adding chloride ions. Although the mechanism still not fully understood, it shows a great prospect. Fluorination, the dipole moment of the perovskite crystal is greatly changed. Figure 34 shows the simple When preparing MAPI, different ratio of MAI and PbI_2 may lead to dramatically different result.

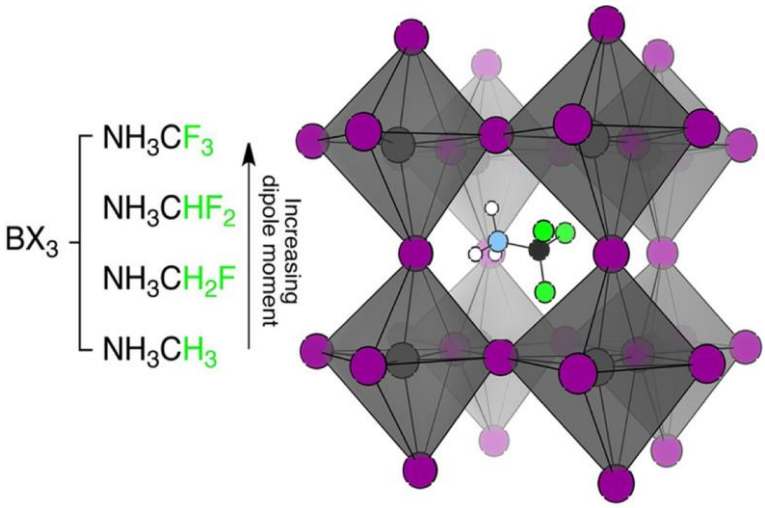

Figure 34: Dipole moment increases when replacing H atom to F atom and shows increasing trend

In the laboratory, the degradation could be easily noticed after few hours and since the perovskite were exposed to ambient room temperature and the moisture. Although light and heat also contribute to the degradation, water is the most critical one. Even though sometimes water can actually enhance the efficiency of perovskite solar cells, it is still wise to avoid the contact with water.

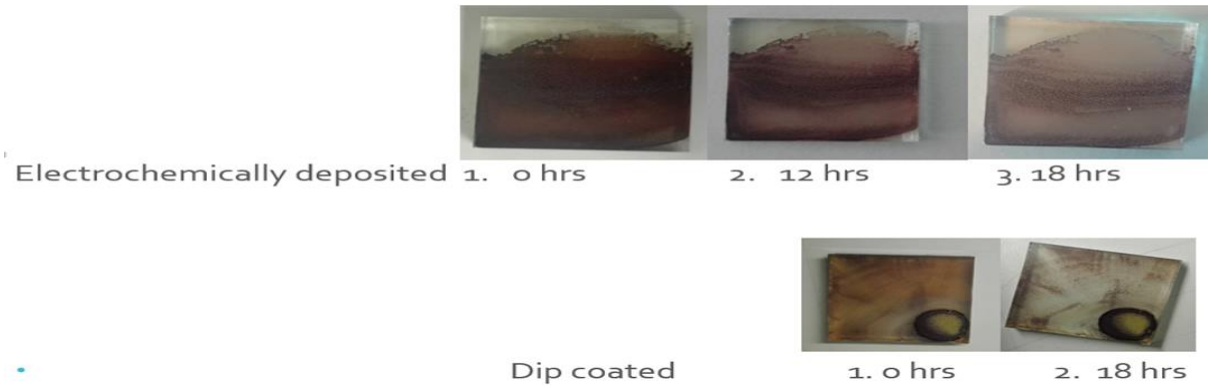

Figure 35: Perovskite formed by dip coating and degraded perovskite after several interval

As seen on figure 35, the degradation starts with the exposure of samples to moisture and even the room temperature. However, the temperature is a strong degrading element and further studies are needed to confirm the trends of degradation. And the degradation site increased in size resulting in the further degradation.

Also, degradation on normal room temperatures and moisture implies a possibility of moisture being integrated into perovskite film since $CH_3NH_3PbI_3$ suffers accelerated degradation under such wet conditions integrated during the manufacturing phase. Perovskite being produced in humid conditions initiates its degradation quicker than the perovskites being processed in dry processed ones.

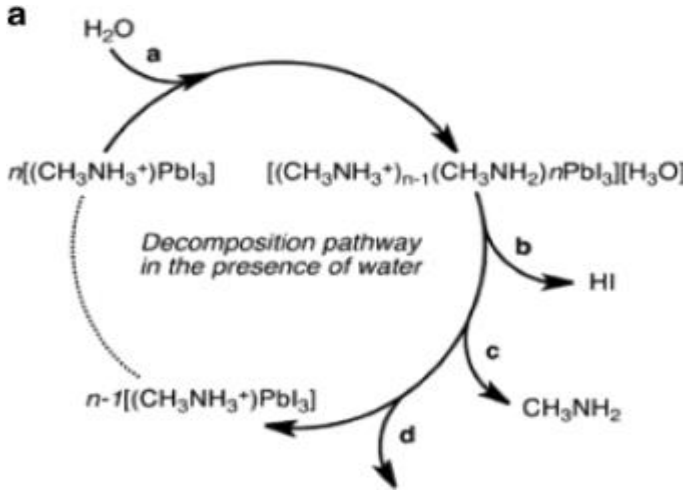

Figure 36 : Moisture initiated perovskite degradation via PbI_2 [2]

Degradation of perovskite also initiates when exposed to elevated temperature via PbI2 and HI.

$CH_3NH_3\,PbI_3 \rightarrow PbI_2 + HI \uparrow + CH_3NH_2 \uparrow$[42]

3.3 Polymer layer protection

PMMA solution prepared was spin coated on top of the perovskite layer followed by the annealing in vacuum oven for 20 min in 80°C and the samples were introduced to Raman microscopy for the morphological studies.

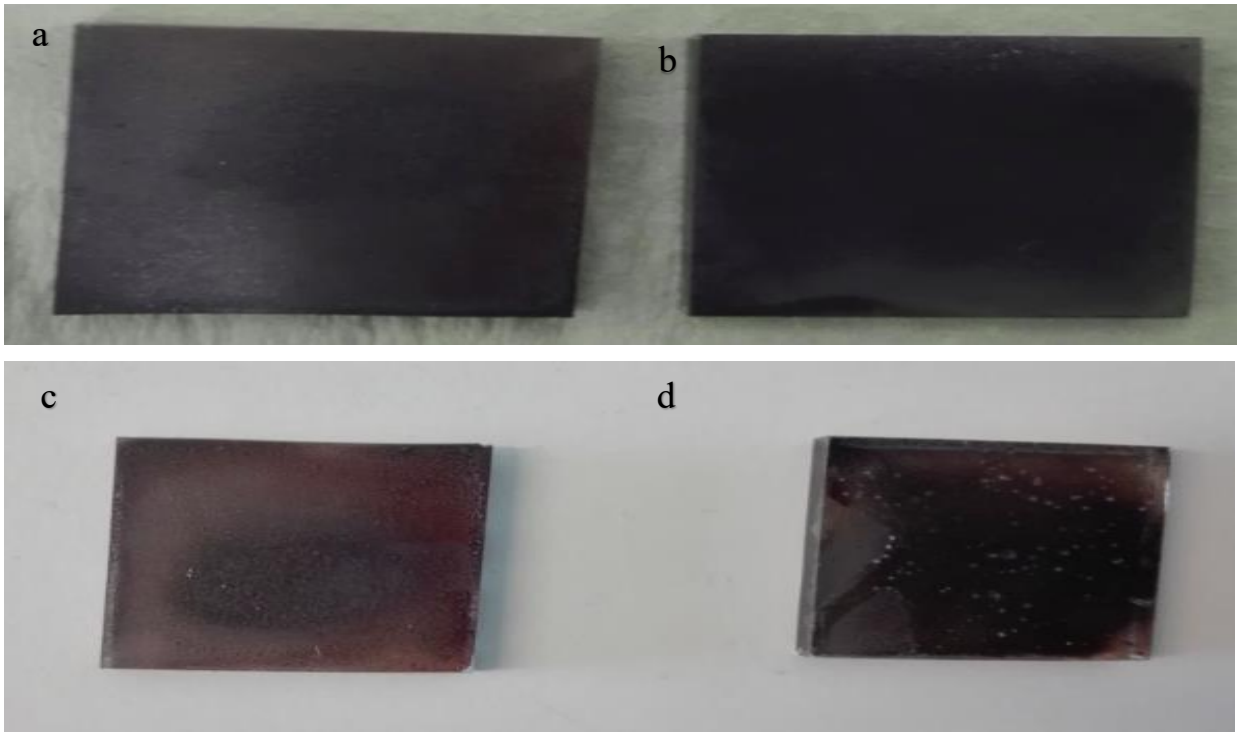

Figure 37: Ultrasonic spray coating prepared perovskites (a) uncoated perovskite and (b) PMMA coated; (c) uncoated perovskite and (d) PMMA coated perovskite appearance after 24 hrs. of normal exposure just after the preparation and after 24 hrs. showing the degradation visibly seen.

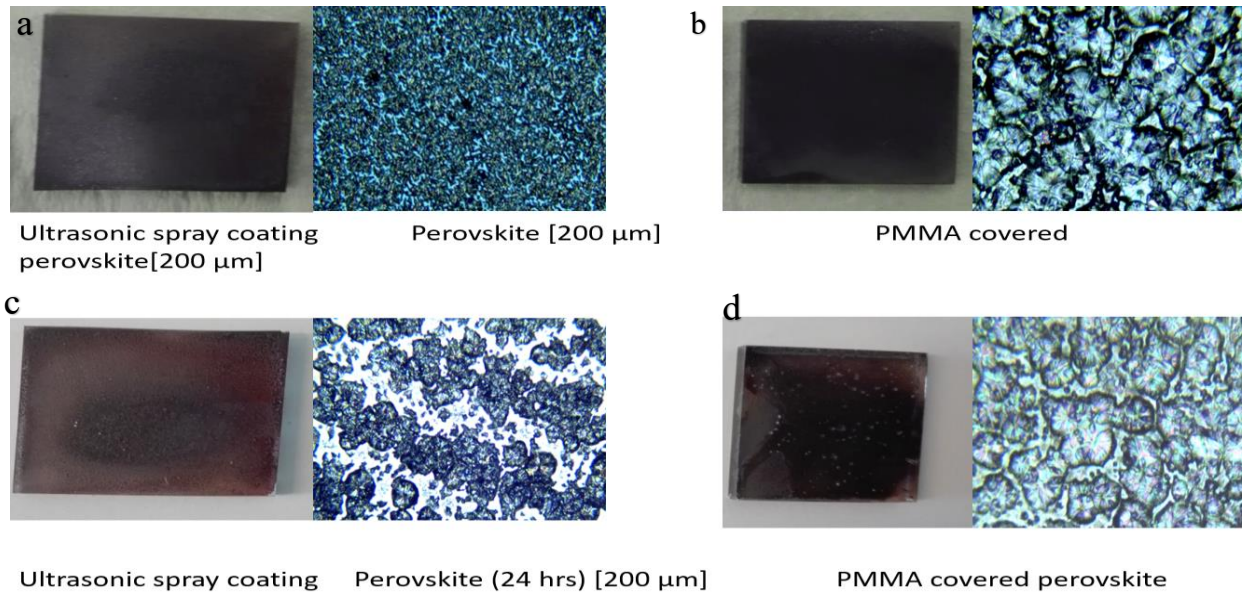

Figure 38: Ultrasonic spray coating prepared perovskites and their respective Raman images (a) uncoated perovskite and (b) PMMA coated; (c) uncoated perovskite and (d) PMMA coated perovskite appearance after 24 hrs. of normal exposure just after the preparation and after 24 hrs.

From the comparisons of the images the degradation is visible to human eye and the Raman microscopic image confirms that avoiding the direct contact of the perovskite with the polymer coating certainly helps in reducing the degradation but still there are some openings for degradations as shown in figure 35(d) and it could be due to the inefficiency during the polymer coating through spin coating.

3.4 Water drop test

To test the polymer layer effect on the perovskite and how it protects the layer, single drop of distilled water was dropped on top of the samples with PMMA layer and without it. The effects could be easily visible with the manual vision.

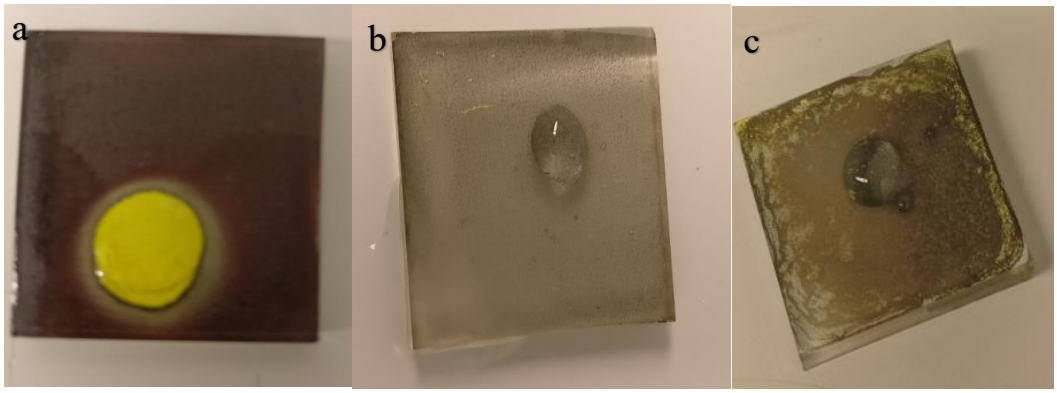

Figure 39: Water drop test on (a) unprotected perovskite layer after 1 hr;(b) water dropped on PMMA covered perovskite after 2 hours and (c) after 2 weeks

Since it could be easily noticed that PMMA will act as the layer to avoid the direct interaction of perovskite with water and prevents from the accelerated degradation via the route of lead iodide. Yellowish colour on perovskite layer in figure 36(a) shows the degradation via lead iodide.

3.5 Spectroscopic studies

3.5.1 *Raman spectroscopy*

Raman spectroscopy can be used for detecting structural and compositional variations for conventional study of photovoltaic applications. Raman studies is powerful, non-contact method for the fundamental and quality control. However, in this thesis, Raman spectra was

used only for the confirmation of the presence of the functional groups on the perovskite and degradation phenomena was just observed manually, microscopic images were studied to get the visible results however only theoretical studies were done for spectroscopic study of the degradation.

Figure 40 shows the Raman peaks for different functional group present in the $CH_3NH_3PbI_3$. Peak at 3003 confirms strongly hydrogen-bonded NH-N= complex occurs resulting in a broad complex set of bands in the 3000-2600 cm^{-1} and intense Raman bands of peak around 970 include the N-radial in-phase stretch in the 1000-980 cm^{-1}. Whereas strong signals at 601,1451 ,2954 represents presence of strong C-I, weak CH_2, CH_3 and N-CH_2 bond interactions respectively which essentially proves the perovskite presence in the sample.

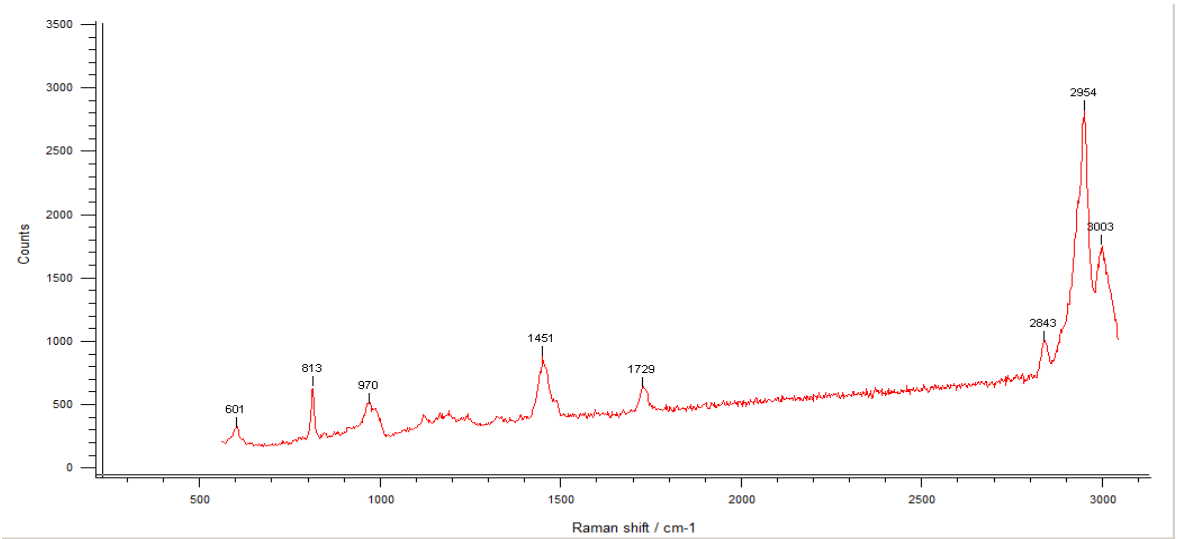

Peak no.	Centre	Height	Width	Area	Absolute intensity	Low edge	High edge
0	1450.96	-	-	-	888.767	-	-
1	812.519	-	-	-	653.48	-	-
2	2953.86	-	-	-	2841.73	-	-
3	3002.65	-	-	-	1771.36	-	-
4	2842.78	-	-	-	1007.74	-	-
5	1728.94	-	-	-	646.775	-	-
6	970.33	-	-	-	518.25	-	-
7	600.582	-	-	-	325.035	-	-

Figure 40: Experimental Raman spectra of $MAPbI_3$ thin films with excitation at 532 nm

As shown and discussed above in figure 33 and 39, $MAPbI_3$ decomposes easily into PbI_2 triggered by moisture and many fundamental properties of the perovskite itself and the constituents during the process of degradation. Decomposition of perovskite $MAPbI_3$ into PbI_2 upon illumination and the atomistic approach explaining this degradation route as the dominant one has been studied. PbI_2, in degraded $MAPbI_3$ coatings could be built upon the excessive illumination and the material instability not only complicates the device fabrication and use but also jeopardizes its characterization[2,54].

From the water drop experiment in figure 39, it can be concluded that the degradation started with the reversible formation of lead iodide from methylammonium lead iodide which was also established theoretically and confirmed with the peak around 120 cm^{-1} during the degradation from spectra which was theoretically concluded[54].

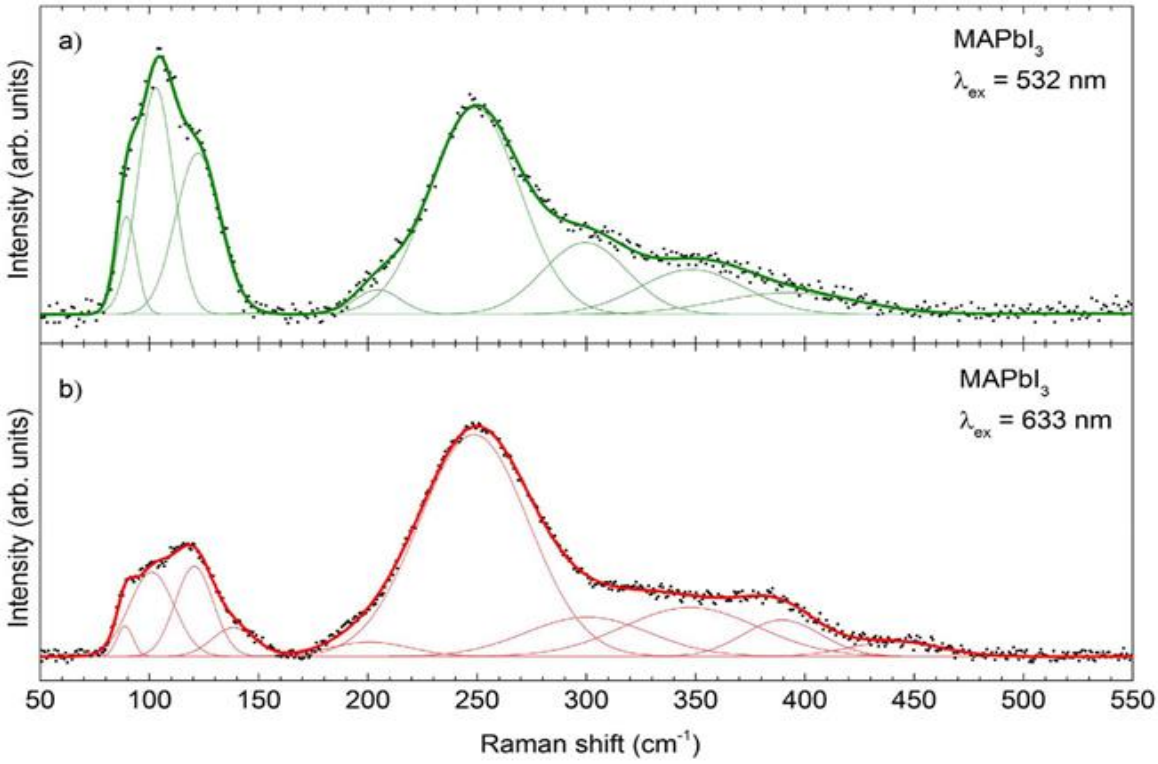

*Figure 41:Theoretical Raman spectra of $MAPbI_3$ thin films with excitation at (**a**) 532 nm and (**b**) 633 nm[54]*

Film thickness, defect densities, composition and crystal structure are the main properties which could be assessed by Raman spectroscopy. Figure 40 shows the Raman spectra of a $MAPbI_3$ film under excitation at 532 nm and keeping the laser power density lower to 26 W/cm^2 in order to avoid thermal effects on the spectrum[54]. This shows the spectra with laser induced degradation sets in, which are characterized by two complex broad structures: one at lower wavenumbers (50–150 cm^{-1}) with other one, even broader contribution at higher wavenumbers (175–450 cm^{-1}).

Degradation study performed also summarizes the peak positions obtained by simultaneous fitting of the spectra during 532 nm and 633 nm excitation peak positions can be compared to values reported in the literature for $MAPbI_3$ and for the PbI_2 phase. Theoretically it has been observed that $MAPbI_3$ thin films degrade, decompose and desorb if excessive laser power densities are used during Raman analysis[54,55].

It has been established an illustrative example is presented how a moderate laser power density of 1300 W/ cm^2 (at 532 nm excitation) leads within seconds to the fast transformation of the $MAPbI_3$ thin films. The new Raman features coincide with the PbI_2 reference it can be noted that PbI_2 rapidly desorb from the substrate. Also, similar effects have been observed when $MAPbI_3$ thin films were studied during heating by real-time X-ray diffraction[50]. Figure 40 explains the continuous monitoring of Raman spectra of a $MAPbI_3$ thin film under the exposure of a moderate laser power density (260 W/cm $^{2)}$. Figure 40 shows the evolution of the Raman spectra with an excitation wavelength of 532 nm as a colour- coded map. In this presentation, each row corresponds to one Raman spectra, where the recorded intensity is coded in a colour-scale. The ordinate represents the time for the laser exposure and the response of the PbI_2 compound for the Raman spectra leads to very intense Raman features and, in consequence, each individual spectrum has been normalized to its maximum in order to distinguish well the different Raman features of all spectra[54]. However, further studies are needed in the future for confirming it.

The degradation of PbI_2 into its polyiodide forms (I_x) is not been clarified at upon additional laser exposure polyiodide compounds. Also, weight factors of the individual phases versus the exposure time, Raman spectra could be beneficial for finding out the duration of the degradation initiation and its continuation into polyiodide compounds. The example stated in the literature illustrates the potential of this methodology to monitor the evolution of different phases with time both qualitatively and quantitatively with further calibration by the method of weight portion determination of the involved phases. However, Raman spectra of polymer coated perovskite samples were not obtained during the thesis.

3.5.2 *Ultra-violet visible spectroscopy interpretation*

UV–vis absorption spectroscopy can be defined as the measurement of the attenuation of a beam of light after it passes through or reflects from a sample surface and it is performed to analyze the light absorption of the bare perovskites and the ones with protected with polymer layer of PMMA and the spectra was studied with absorbance vs wavelength spectra. In perovskite solar cells, one of the factors determining if the solar cell works is the light absorption by the light absorber material which clearly states the importance of UV-Vis spectra in this field[27,29].

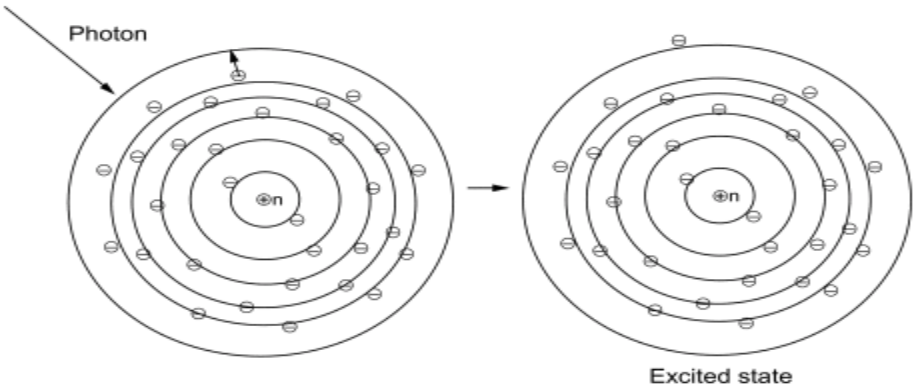

Figure 42: Basics of absorption spectra [27]

Absorptions spectra was examined using regular ultraviolet-visible light for wavelengths up to 1200nm and the phenomena of UV-Vis is that when the sample is illuminated with light an electron is excited corresponding to the energy difference between an electronic transition (for example bonding to anti-bonding) inside the molecules. The light is absorbed and the absorption of the sample is shown as a graph at different wavelengths [27,28].

In this project this methodology has been used to investigate the processes for charge generation and hole transfer in both lead based perovskites and the PMMA coated perovskite for the study of impact of polymer layer coating on its degradation. The studies are in this case to measure the change in absorption both with and without adding PMMA. When a pulsed light beam of 530 nm green light emitted by a laser LED, excites the sample constituting perovskite coated on FTO sample and PMMA coating the perovskite on top of it. Then the white "probe light" beam analyzes the excited sample and light is sent through the sample to the monochromator and detection occurs using either a Si or Ge photodiode, and respective spectra were obtained in the computer screen.

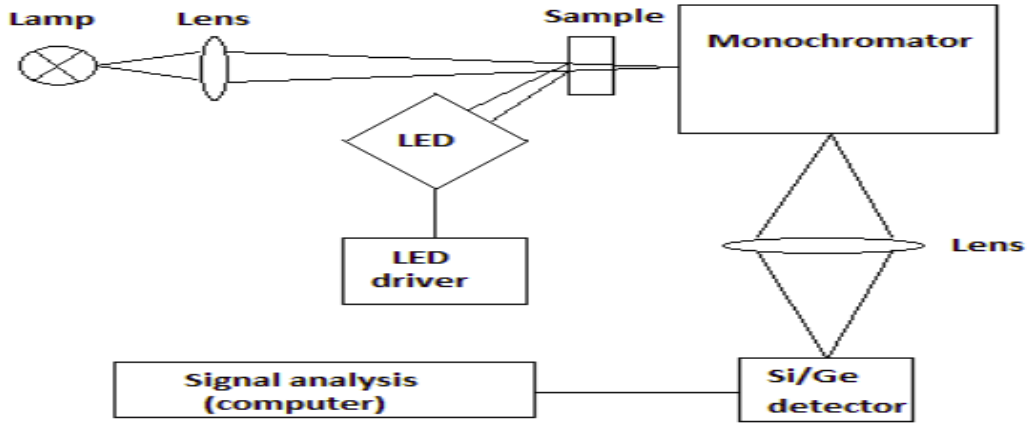

Figure 43: Demonstration of functional parts in a photo-induced absorptions instrument [27]

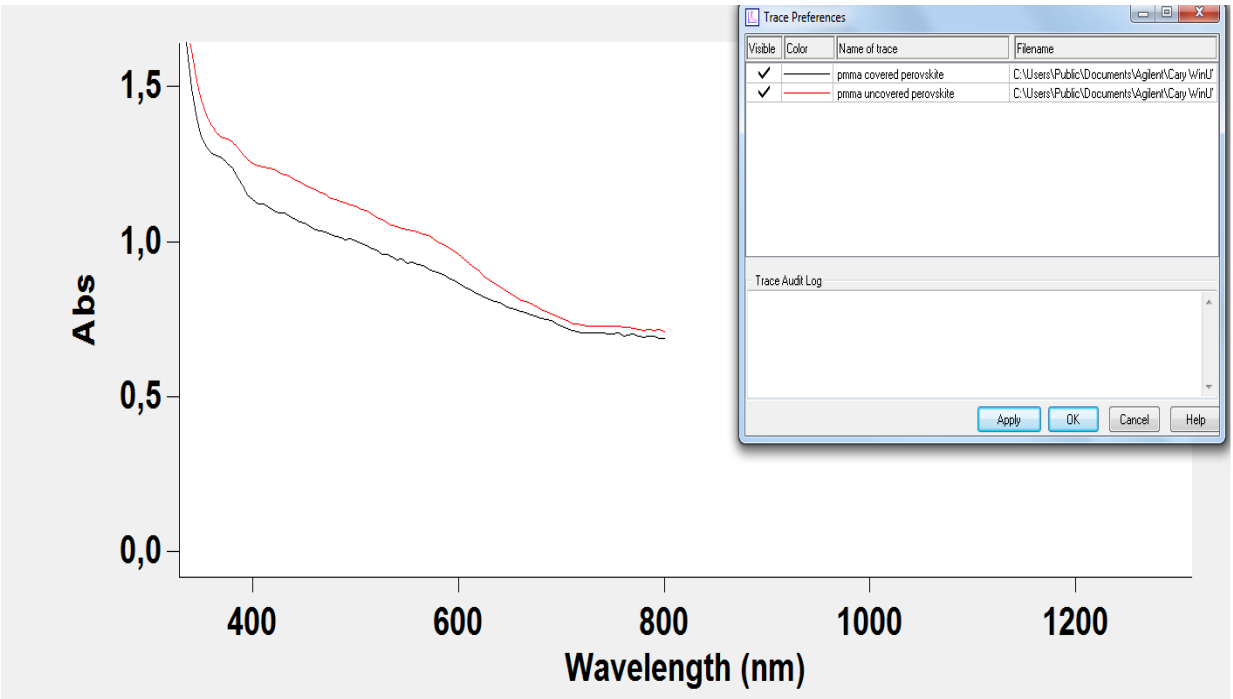

Figure 44: Absorption vs wavelength UV-vis spectra of perovskite formed by ultrasonic spray coating and PMMA coated on top of it.

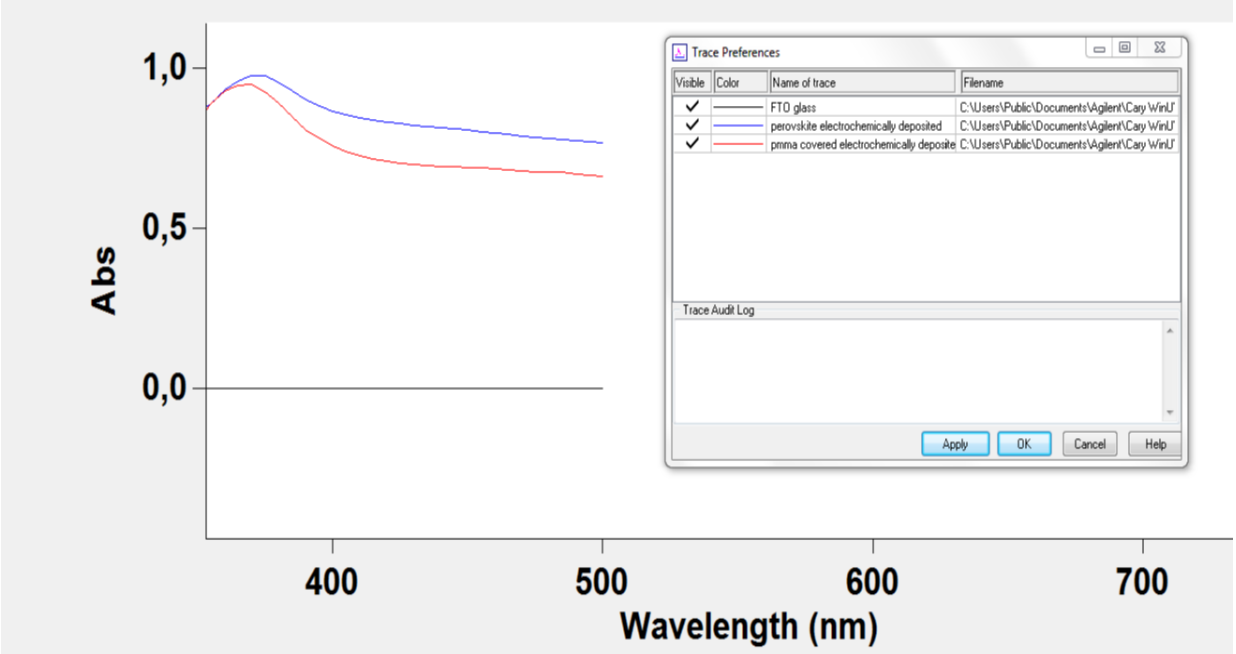

Figure 45: Absorption vs wavelength UV-vis spectra of perovskite formed by electrochemical deposition and PMMA coated on top of it

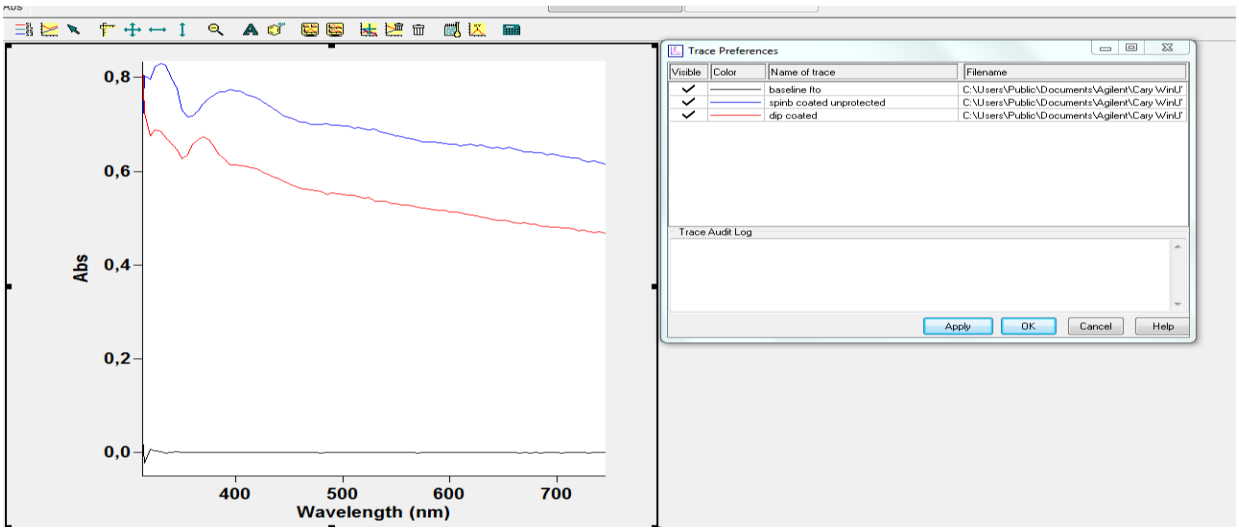

Figure 46: Absorption vs wavelength UV-vis spectra of perovskite formed by dip coating and PMMA coated on top of it.

In all of the three spectra in figure [45-47], it is clear that the absorption of the photon energy is high on the bare perovskite layer whereas if the same sample is coated (protected) with PMMA layer the impact of the photon energy has been reduced. Also, during the water drop test in this thesis as shown in figure [39], PMMA act as a protecting layer for perovskite layer from ambient temperature and moisture. However, the polymer layer material has to be studied along with its impact of the polymer layer on the device performance as a whole has to be evaluated for future researches[56].

4. Conclusion

As clarified on whole research, potential of perovskite materials is so huge that it could disrupt current photovoltaics landscape. Efficiency increment in recent years with its device performance is encouraging but there are still many areas of the material which can be enhanced for its commercial use. Alternatively, it has been stated that coupling of perovskite material with currently available silicon solar cells could maximize to form the high efficiency tandem cells. Stability however has been a key barrier for its approach to the market as a commercially viable product[2].

Instability of hybrid perovskite solar cell due to the exposure to moisture is a primary concern for its growth and to find the stable perovskite material by altering the elements in ABX_3 structure. The key factors like irradiation with UV light and thermal decomposition could also be impacted by alternating the materials in perovskite structure[41,43].

Different studies could however be done for the stability of current perovskite material in different conditions of controlled N_2 environment in a glovebox which could help in finding the ideal lifetime of currently feasible perovskite-based photovoltaics. Research on perovskite material is required to be based upon the performance of the whole system rather than just the individual layer stability[2].

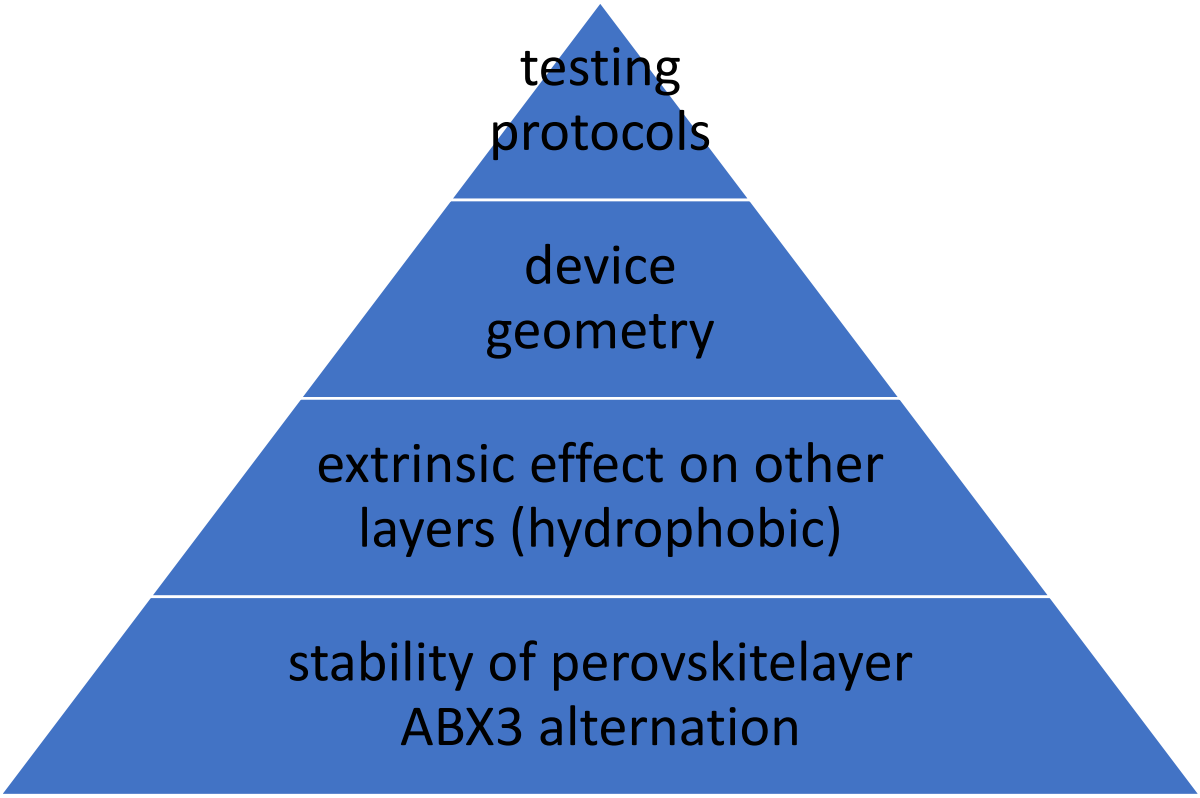

Figure 47: Perovskite solar cell fabrication with regards to future research [2]

The device performance as a whole system should be looked upon for the stability of the system and for that every layer starting from bottom one should be hydrophobic. Charge transport layer atop the perovskite absorber should be hydrophobic to avoid the direct exposure to moisture and resulting in the reduced moisture ingress to the perovskite. As established on this thesis, PMMA as being hydrophobic protects the moisture accelerated degradation of perovskite. For the device to be working, metal electrode used for the device fabrication should be cost effective and stable which shows the problem of using silver (Ag) for instability and gold (Au) for its ineffectiveness in cost. Carbon ink has been looked upon as an ideal replacement for the metal electrode and more researches need to be done for an end result to be successful[2,54].

For the spectroscopic studies , conclusions that could be made are the spectroscopic methods has to be further applied to layered structures to obtain meaningful spectra from buried layers as long as the top layers are transparent to the used laser excitation and the Raman studies of the whole solar cells by selecting the appropriate excitation wavelength[24] could be beneficial to understand opto-electronic and performance parameters of the device, enabling a powerful quality and possibly degradation control. It has to be noted that use of Raman spectroscopy is really beneficial to detect and monitor degradation in perovskite solar cells as it is an contactless, non-destructive, in order to obtain meaningful Raman spectra of $MAPbI_3$ thin films at low laser power densities. Since it has been already stated in literatures the importance of choosing a relevant excitation wavelength of Raman has to be respected as and an excitation at 633 nm was shown to be less harmful than excitation at 532 nm[54].

Also, along with instability of the perovskite material there are also some other challenges of using perovskite material which need to be considered for future research for efficient commercial application. Eco toxicity problems posed by Pb as it has been stated in the MAI contributes more to negative environmental impacts when compared to $PbCl_2$ Further studies on the materials which is more greener element and could replace Pb from perovskite could be helpful in reducing the current uncertainty surrounding this issue[22].

Since theoretical efficiency achieved for perovskite cells are already on par with inorganic thin-film technologies thus the shift has to be moved towards achieving the efficiency on commercial field and along with improving their long-term stability. From the experiment conducted in this thesis it can also be concluded that the inherent instability of $MAPbI_3$ towards moisture and oxygen can be manipulated by introducing functional barrier layers into the device structures allowing efficient charge extraction while minimizing the ingress of degradation agents. However, the impact on the device stability has to be evaluated. Also, as a polymer been applied on the thesis it appears that the polymer layer delays the degradation rather than preventing it. Thus, for the device performance it could be in best interest of all that the perovskite absorber stabilizes itself by substituting its constituent ions as mixed cation and mixed halide compositions, as well as lower-dimensional structures, show very promising results[2,57].

For the perovskite structure manipulation the weak point of the perovskite is the A-site cation as methylammonium is too volatile to be retained in the perovskite structure when exposed to external stressors and replacing MAI with alternatives like formamidinium and cesium might be beneficial to give the perovskite much better stability and further researches need to be done as this structures can only be stabilized in the right phase when present as ionic mixtures[51]. The impact of this functional groups on charge-selective layers, either inorganic or inert organic layers, and mature encapsulation techniques in order to survive true long-term stability studies has to be studied along with the systematic stress tests such as high-humidity and full-temperature cycles, which could be an important gauge for the maturity of this photovoltaic technology[2,22,41].

Finally, for testing protocols considering that the perovskite absorber is so sensitive to moisture that the testing under "ambient" conditions becomes really problematic. The studies that could be done are the surface morphology through different microscopic features including SEM and Raman microscopy. Degradation phases and element acquisition could be performed by Raman spectroscopy and absorption properties of the materials could be performed by the UV-vis spectroscopy[2].

5. References

1. Kazici, M. *et al.* Solar Cells. in *Comprehensive Energy Systems* (2018). doi:10.1016/B978-0-12-809597-3.00426-0
2. Wang, D., Wright, M., Elumalai, N. K. & Uddin, A. Stability of perovskite solar cells. *Sol. Energy Mater. Sol. Cells* **147**, 255–275 (2016).
3. Pandey, C., Klemetti, A. & Asghar, M. I. Application of Printing Techniques in Hybrid Photovoltaic Technologies. (2015).
4. Uddin, A. *Perovskite Solar Cells*. (2018). doi:10.1142/9789813239494_0009
5. Spanggaard, H. & Krebs, F. C. A brief history of the development of organic and polymeric photovoltaics. *Sol. Energy Mater. Sol. Cells* (2004). doi:10.1016/j.solmat.2004.02.021
6. Green, M. A. High-efficiency silicon solar cell concepts. in *McEvoy's Handbook of Photovoltaics: Fundamentals and Applications* (2017). doi:10.1016/B978-0-12-809921-6.00005-7
7. Badawy, W. A. A review on solar cells from Si-single crystals to porous materials and Quantum dots. *Journal of Advanced Research* (2015). doi:10.1016/j.jare.2013.10.001
8. Tvrdy, K. & Kamat, P. V. Quantum Dot Solar Cells. in *Comprehensive Nanoscience and Technology* (2010). doi:10.1016/B978-0-12-374396-1.00129-X
9. Green, M. A. Third generation photovoltaics: Solar cells for 2020 and beyond. in *Physica E: Low-Dimensional Systems and Nanostructures* (2002). doi:10.1016/S1386-9477(02)00361-2
10. barry tonkin. SunPowerSource - SunPowerSource types of solar panels. Available at: https://www.sunpowersource.com/types-of-solar-panels/. (Accessed: 15th May 2019)
11. Kim, J., Lee, S. H., Lee, J. H. & Hong, K. H. The role of intrinsic defects in methylammonium lead iodide perovskite. *J. Phys. Chem. Lett.* (2014). doi:10.1021/jz500370k
12. Emerging High-Efficiency Low-Cost Solar Cell Technologies - ppt video online download. Available at: https://slideplayer.com/slide/5386641/. (Accessed: 15th May 2019)
13. Noh, J. H., Im, S. H., Heo, J. H., Mandal, T. N. & Seok, S. Il. Chemical management for colorful, efficient, and stable inorganic-organic hybrid nanostructured solar cells. *Nano*

Lett. (2013). doi:10.1021/nl400349b

14. Song, Y. H. *et al.* Design of water stable green-emitting CH3NH3PbBr3 perovskite luminescence materials with encapsulation for applications in optoelectronic device. *Chem. Eng. J.* **306**, 791–795 (2016).

15. Gonzalez-Pedro, V. *et al.* General working principles of CH3NH3PbX3 perovskite solar cells. *Nano Lett.* (2014). doi:10.1021/nl404252e

16. Tzounis, L. *et al.* Perovskite solar cells from small scale spin coating process towards roll-to-roll printing: Optical and Morphological studies. *Mater. Today Proc.* **4**, 5082–5089 (2017).

17. Lee, J. W., Na, S. I. & Kim, S. S. Efficient spin-coating-free planar heterojunction perovskite solar cells fabricated with successive brush-painting. *J. Power Sources* **339**, 33–40 (2017).

18. Samu, G. F., Scheidt, R. A., Kamat, P. V. & Janáky, C. Electrochemistry and Spectroelectrochemistry of Lead Halide Perovskite Films: Materials Science Aspects and Boundary Conditions. *Chem. Mater.* **30**, 561–569 (2018).

19. Khalil, M., Wang, S., Yu, J., Lee, R. L. & Liu, N. Electrodeposition of Iridium Oxide Nanoparticles for pH Sensing Electrodes. *J. Electrochem. Soc.* **163**, B485–B490 (2016).

20. Kajal, P. & Powar, S. Applications of solar energy. *Nature* **191**, 228 (1961).

21. Rout, T., Bera, S., Udayabhanu, G. & Narayan, R. Methodologies of Application of Sol-Gel Based Solution onto Substrate: A Review. *J. Coat. Sci. Technol.* **3**, 9–22 (2016).

22. Rong, Y., Liu, L., Mei, A., Li, X. & Han, H. Beyond efficiency: The challenge of stability in mesoscopic perovskite solar cells. *Advanced Energy Materials* (2015). doi:10.1002/aenm.201501066

23. Schrader, B. *Frontmatter*. *Infrared and Raman Spectroscopy* doi:10.1002/9783527615438.fmatter

24. John, N. & George, S. Raman Spectroscopy. in *Spectroscopic Methods for Nanomaterials Characterization* (2017). doi:10.1016/B978-0-323-46140-5.00005-4

25. *Introductory Raman Spectroscopy*. *Introductory Raman Spectroscopy* (2016). doi:10.1016/b978-0-12-254105-6.x5000-8

26. Scientific, H. a plic tion Note Forensics The non destructive and in-situ identification of different black inks. 1–2

27. Braeuer, A. Absorption Spectroscopy. in *Supercritical Fluid Science and Technology*

(2015). doi:10.1016/B978-0-444-63422-1.00006-7

28. MASAGO, H. *UV/Vis spectroscopy*. *Journal of the Japan Society of Colour Material* **78**, (2015).

29. UV-VIS spectroscopy and its applications. *Choice Rev. Online* (2013). doi:10.5860/choice.30-6183

30. Troughton, J., Hooper, K. & Watson, T. M. Humidity resistant fabrication of CH3NH3PbI3 perovskite solar cells and modules. *Nano Energy* **39**, 60–68 (2017).

31. Schwartz, R. W. Chemical Solution Deposition of Perovskite Thin Films. *Chemistry of Materials* (1997). doi:10.1021/cm970286f

32. Aguilar, R. G. & López, J. O. Low cost instrumentation for spin-coating deposition of thin films in an undergraduate laboratory. *Latin-American J. Phys. Educ.* **5**, 368–373 (2011).

33. Paunovic, M. & Schlesinger, M. *Fundamentals of Electrochemical Deposition: Second Edition*. *Fundamentals of Electrochemical Deposition: Second Edition* (2005). doi:10.1002/0470009403

34. Chen, H. Two-Step Sequential Deposition of Organometal Halide Perovskite for Photovoltaic Application. *Adv. Funct. Mater.* **27**, (2017).

35. Pellet, N. Thesis - Investigations on hybrid organic-inorganic perovskites for high performance solar cells. *EPFL Thesis* **7749**, 1–248 (2017).

36. Paridah, M. . *et al.* We are IntechOpen , the world ' s leading publisher of Open Access books Built by scientists , for scientists TOP 1 %. *Intech* **i**, 13 (2016).

37. Costa Milan, D. Experimental study of electronic transport in single molecular contacts and surface modification via STM. 1 (2016). doi:10.13140/RG.2.1.1560.9844

38. ALVES, B. & CAMPBELL, B. Golden Rain. *Lou Harrison* 327–340 (2018). doi:10.2307/j.ctt1zxz014.40

39. Das, S. *et al.* High-Performance Flexible Perovskite Solar Cells by Using a Combination of Ultrasonic Spray-Coating and Low Thermal Budget Photonic Curing. *ACS Photonics* **2**, 680–686 (2015).

40. Sánchez-Herencia, A. J. Water based colloidal processing of ceramic laminates. *Key Eng. Mater.* **333**, 39–48 (2007).

41. Niu, G. *et al.* Study on the stability of CH3NH3PbI3 films and the effect of post-modification by aluminum oxide in all-solid-state hybrid solar cells. *J. Mater. Chem. A*

(2014). doi:10.1039/c3ta13606j

42. Yang, J., Siempelkamp, B. D., Liu, D. & Kelly, T. L. Investigation of CH3NH3PbI3degradation rates and mechanisms in controlled humidity environments using in situ techniques. *ACS Nano* (2015). doi:10.1021/nn506864k

43. Park, N. G. Perovskite solar cells: An emerging photovoltaic technology. *Materials Today* (2015). doi:10.1016/j.mattod.2014.07.007

44. Semaltianos, N. G. Spin-coated PMMA films. *Microelectronics J.* (2007). doi:10.1016/j.mejo.2007.04.019

45. Bornside, D. E. Spin Coating of a PMMA/Chlorobenzene Solution. *J. Electrochem. Soc.* (1991). doi:10.1149/1.2085563

46. Spin Coating. Available at: https://www.slideshare.net/krishslide/spin-coating-39462865. (Accessed: 15th May 2019)

47. Sheng Hsiung Chang, Chien-Hung Chiang, Feng-Sheng Kao, Chuen-Lin Tien & Chun-Guey Wu. Unraveling the Enhanced Electrical Conductivity of PEDOT:PSS Thin Films for ITO-Free Organic Photovoltaics. *IEEE Photonics J.* **6**, 1–7 (2014).

48. Kahlert, H. Reference electrodes. in *Electroanalytical Methods: Guide to Experiments and Applications* (2010). doi:10.1007/978-3-642-02915-8_15

49. Krebs, F. C. Fabrication and processing of polymer solar cells: A review of printing and coating techniques. *Solar Energy Materials and Solar Cells* (2009). doi:10.1016/j.solmat.2008.10.004

50. Eslamian, M., Soltani-Kordshuli, F. & Binda, M. Deposition and patterning techniques for Organic Semiconductors Solution processable materials : deposition techniques. *Org. Electron. Princ. Devices Appl.* (2011). doi:10.1007/s11998-017-9975-9

51. Hellier, K. *et al.* Mechanisms for light induced degradation in MAPbI 3 perovskite thin films and solar cells . *Appl. Phys. Lett.* **109**, 233905 (2016).

52. Yang, J. & Kelly, T. L. Decomposition and Cell Failure Mechanisms in Lead Halide Perovskite Solar Cells. *Inorganic Chemistry* (2017). doi:10.1021/acs.inorgchem.6b01307

53. Kang, S. J. *Sintering*. *Sintering* (2005). doi:10.1016/B978-0-7506-6385-4.X5000-6

54. Pistor, P., Ruiz, A., Cabot, A. & Izquierdo-Roca, V. Advanced Raman Spectroscopy of Methylammonium Lead Iodide: Development of a Non-destructive Characterisation Methodology. *Sci. Rep.* **6**, 1–8 (2016).

55. Zhou, Y., Garces, H. F. & Padture, N. P. Challenges in the ambient Raman spectroscopy

characterization of methylammonium lead triiodide perovskite thin films. *Front. Optoelectron.* **9**, 81–86 (2016).

56. Picollo, M., Aceto, M. & Vitorino, T. UV-Vis spectroscopy. *Phys. Sci. Rev.* (2018). doi:10.1515/psr-2018-0008

57. Grill, I. *et al.* Controlling crystal growth by chloride-assisted synthesis: Towards optimized charge transport in hybrid halide perovskites. *Sol. Energy Mater. Sol. Cells* **166**, 269–275 (2017).